ISSN: 2634 - 8845

Journal of Earth and Environmental Science Research

SCIENTIFIC Research and Community

Review Article

Open Access

Gravitational Radiation Induced Spiral-in Offsets the Pulsar Pair from its Final Lock-in Position- a New Metric for Relativistic Pulsar Binaries

Bijay Kumar Sharma

Ex-Emeritus Fellow, Electronics & Communication Department, National Institute of Technology, Patna -800005, Indian Institute of Technology Patna, India

ABSTRACT

Author has extensively studied Earth-Moon system, Phobos-Mars system, Deimos-Mars System, Charon-Pluto system and Iapetus-Saturn system and developed Kinematic Model (KM) of tidally interacting binary systems. KM predicts two Geo-synchronous orbits aG1 and aG2 in case of Earth-Moon system and two Clarke's orbits aG1 and aG2 in case of Phobos-Mars system, Deimos-Mars System, Charon-Pluto system and Iapetus-Saturn system. The secondary of the tidally interacting is always born at aG1 but aG1 is total energy maxima hence the secondary is in an unstable equilibrium state and any perturbing force nudges the secondary either short of aG1 or long of aG1. If the secondary falls short of aG1 the secondary is launched on a gravitational runaway collapsing sub-synchronous spiral path destined to make a glancing collision with the primary if the secondary does not get pulverized after entering the Roche's limit of the primary as is the case with Phobos with respect to Mars. If the secondary falls long of aG1 as is the case with Earth-Moon system or Pluto-Charon system, the secondary experiences a powerful gravitational sling shot impulsive torque and secondary gets launched on an expanding spiral path with a radial recessive velocity. Eventually secondary gets tidally locked in a triple synchrony state [$T_{spin\_primary} = T_{spin\_secondary} = T_b$ (orbital period)] with zero radial velocity of recession. This is the case with Pluto-Charon. While describing these tidally interacting binaries there are three relevant parameters: 'q' = ratio of secondary to primary mass, time constant of evolution $\tau = \frac{aG2-aG1}{V_{max}}$ where V_{max} = the maximum velocity experienced by the secondary at a semi-major axis a1 the point of maximm impulsive torque during 'gravitational sling shot' and evolution factor $= \frac{a-aG1}{aG2-aG1}$ where 'a' is the current semi major axis of the secondary. KM states that if 'q' is less than 0.0001 that is the mass ratio is infinitesimal as is the case with artificial geo-synchronous satellites, the man-made geo-synchronous satellite is trapped in 36,000 Km synchronous orbit above the equator of Earth with geo-stationary position with resect to Earth's surface. When 'q' is less than 0.0001, then time constant of evolutions is infinite, evolution factor is zero and the second art is stay put in aG1 orbit. When 0.001 <q <0.2 then secondary has a finite time constant of evolution from Gy to Ky in inverse proportion to some power of 'q' and evolution factor is 0 to Unity. When 0.2 <q <1 evolution factor approaches UNITY and secondary settles in aG2 orbit in years, months and days. Pluto Charon, Brown Dwarf pairs and star pairs up to White Dwarfs state are examples of this. But as we go to Neutron Star pairs or Neutron Star and Black Hole pairs or Black Hole pairs, we enter high gravitational field regime and Gravitational Radiation is induced which results in Gravitational Radiation induced spiral-in and hence offseted from the final lockin position at aG2. The strength of relativity is decided by the APSIDAL MOTION or the rate of periastron advance. Higher is the apsidal motion of relativistic pair, higher is 'the offset' from final locking position. This is precisely the finding of this paper. 6 Double Neutron Star Binaries (DNSBs) namely PSR J1811-1736, PSR J1518+4904, PSR B1534+12, PSR B1913+16(Hulse-Taylor Pair), PSR 2127+11C and PSR J0737-3039 are tested for KM prediction of Unity Evolution Factor. This off-set with respect to final lock-in is in proportion to the relativistic strength of the DNSB measured by apsidal motion or rate of periastron advance. In this paper Keplerian Binaries such as Main Sequence Star Binary RW Lacerate, M Dwarf-White Dwarf pre-cataclysmic NN Serpentis are also studied as examples of non-relativistic binaries. Main Sequence Star Binary RW Lacerate and M Dwarf-White Dwarf pre-cataclysmic NN Serpentis are found to be in outer Clarke's Configuration with triple synchrony state achieved as predicted.

***Corresponding author**

Bijay Kumar Sharma, Ex-Emeritus Fellow, Electronics & Communication Department, National Institute of Technology, Patna -800005, Indian Institute of Technology Patna, Bihta Campus – 801118, India.

Received: June 19, 2024; **Accepted:** June 22, 2024; **Published:** July 15, 2024

Keywords: Gravitational Waves, Astrometry, Star Binaries, Spectroscopic, Star Pulsars, General Survey, Apsidal Motion

The Gravitational Sling Shot Model of Earth-Moon

In 18th Century, German Philosopher Kant had suggested the theory of retardation of Earth's spin based on the ancient records of Solar Eclipses [1,2]. Similar kind of studies have been carried out by Kevin Pang at Jet propulsion Laboratory at Pasadena [3,4]. He happened to step upon certain ancient records regarding Solar Eclipses. A total Solar Eclipse had been observed in the town of Anyang, in Eastern China, on June 5, 1302 B.C. during the reign of Wu Ding. Had Earth maintained the present rate of spin, the Eclipse should have been observed in middle of Europe. This implies that in 1302 B.C. i.e. 3,291 years ago Earth's spin period was shorter by 0.047 seconds. This leads to a slowdown rate of 1.428 seconds per 100,000 years.

In 1879 George Howard Darwin carried out a complete theoretical analysis of Earth-Moon System and put forward a sound hypothesis for explaining the slowdown of Earth's spin on its axis.

According to George Howard Darwin (son of Charles Darwin, father of Evolution Theory), Moon is the daughter of the Earth [5,6]. At the time of birth of the Solar System, when Earth was accreted from circumstellar disc of gas and dust, Earth was born with a initial spin period of 8 days in synchrony with the fiducial spin period of Sun which was 8 days at the formation age 650My after the birth of the Solar Nebula [7,8]. Earth's triple synchrony with Sun is in accordance with the New Perspective on the birth and evolution of the Solar System presented at 35th COSPAR Scientific Assembly [9]. Here triple synchrony implies that:
$P_{spin\_Sun} = P_{spin\_Earth} = P_{orb\_Earth} = 8$ days.

Subsequently through a series of minor impacts with the residual planetesimals, Earth was spun-up to a period of 5 hours.

At the time of birth, Earth had no natural satellites. Hence Solar tides were the only tidal force. For an Earth-day of 5 hours at the beginning of times, Solar- tides came and ebbed at 2.5 hours interval. The Solar tides created a forced vibration of Earth's bulk at the frequency of 0.4 cycles per hr. George calculated the natural frequency of vibration which came out to be [SOM_Appedix H]

$$\sqrt{\frac{GM_{+}}{4R^3}} = \frac{2\pi}{P_{nat}} \qquad 1$$

Where R = radius of the Earth $=6.37814\times10^{6}$ m;
M_{+} = mass of the Earth $=5.9742\times10^{24}$Kg;
Solving this Equation 1, we get the natural period of vibration as 2.8 hours which corrected for the stratified Earth comes to be 2.5 hours which is the same as the forced frequency of vibration.

In course of spin-up due to minor impacts, as soon as the solar tide forced vibration time period was coincident with the Earth's bulk natural time period, resonance occurred. This led to exponential increase in the amplitude of vibrations along the oblate and prolate axis. The Sun's tides were alternately stretching and squeezing the Earth. As the amplitude of vibrations increased to 14,626 Km the tidally oscillating Earth was transformed into an attached binary with a tenuous link at the apex of Roche's lobe. The link got broken and the secondary component got placed in an orbit of 14,626Km and the remnant Earth continued to spin at 5 hours period. This secondary component became our Moon and both the Earth and the Moon were tidally interlocked because 14,626Km was the inner geosynchronous orbit.

The Roche's limit for Earth and Moon is 18,000Km hence Moon got tidally pulverized and there was a circumterrestrial disc of debris from which Moon was accreted in Roche's zone from 14,797Km to 24,740Km. Fully merged Moon was formed and reborn just beyond 18,000Km [10].

George postulated that Moon was torn out of the Pacific Ocean basin and hurled onto an outward spiral trajectory. The point of formation must have been Roche's Limit which is 18,000Km and this is greater than the inner geosynchronous orbit 14,626Km hence Moon was in super-synchronous orbit tidally retarding Earth's spin of 5 hours period and Moon itself receding from the Earth [personal communication: http://arXiv.org/abs/0805.0100]. Today Earth's spin has slowed down from 5 hours to 24 hours and Moon has receded from 18,000Km orbital radius to the present-day orbital radius of 384,400Km.

Once Earth-Moon System is born, because of proximity, lunar tides became the dominating tidal force and it drove the System off-resonance.

George postulated that Moon was orbiting at an angular velocity Ω which was slower than the spin angular velocity ω of the Earth. Hence slow orbiting Moon tries to hold back Earth's spin. This leads to a transfer of angular momentum from fast spinning Earth to slow orbiting Moon. This results in outward spiral orbit of Moon and tidal braking of the rapidly spinning Earth.

The lunar tidal torque slows down the fast spinning Earth. Simultaneously Moon gets pushed outward until the two bodies become geo-synchronous. George calculated that the final geo-synchronous orbit aG will be 1.5 times the present Lunar Orbital Radius of $a_P = 3.844\times10^{8}$m i.e. $a_G = 5.766\times10^{8}$m. George also calculated the geo-synchronism period to be 47 days. That is Solar Day on Earth will be 47 days long and there will be no Moon Rise or Moon Set. This will be a state of triple synchrony where $P_{spin\_Moon} = P_{Orb\_Moon} = P_{spin\_Earth} = 47$ days.

George further postulated that after geo-synchronism is achieved, Solar tidal drag will become dominant. Sun will try to bring Earth in synchronous orbit as Moon is in synchronous orbit around Earth.

Moon's synchronism with respect to Earth means Moon's orbital velocity and Moon's spin velocity are equal leading to Moon keeping the same face towards Earth all the time [11]. As a result, we see only one side of Moon. The other side always remains in dark. In 1959 Russian Luna probes for the first time photographed the dark side of Moon.

Further retardation of Earth's spin velocity by Sun's tidal interaction with respect to Moon's orbital velocity will lead to reversal of transfer of angular momentum. Now lunar tidal interaction will try to make Earth spin faster and angular momentum will be transferred from Moon to Earth. As a result Moon will be drawn into a collapsing or inward spiral orbit ultimately leading to head on collision of Moon into Earth [12,13].

Much earlier than this doomsday, our Sun would have consumed its fusion fuel and left the main sequence to become Red Giant and then collapse into a White dwarf. As our Sun bloats into Red Giant a few billion years hence, it would devour the terrestrial Planets including Earth-Moon System [14,15].

Hence Earth would never survive to meet the fateful and devastating head on collision with Moon.

As Author writes this paper new evidence show that Moon is indeed the daughter of our Earth as proposed by George Howard Darwin originally based on isotopic composition similarity [16]. New simulation results by show that "an erosive giant impact onto a fast spinning proto-earth followed by de-spinning during passage through the evection resonance can reproduce the isotopic homogeneity and the present angular momentum of Earth-Moon System" [17]. This simulation has combined Hartmann's Giant Impact with the Fission Hypothesis first proposed by George Howard Darwin.

Modern Findings about Moon

Since George Howard Darwin proposed his Hypothesis, Human-Kind has made spectacular progress in every field of Science and Technology including the field of Astronomy and Astrophysics. The launching of Astronomical Satellites has helped us make

precise measurements of different orbital and globe parameters of various Celestial Objects of interest [18].

Ranger Probes have pinned down the value of mG of our Moon at 4902.78±0.05 $(km)^3/(sec)^2$. The ratio of masses of Moon and Earth have been improved 30 fold. This has been achieved by tracking the motion of Earth around the barycenter of Earth-Moon System. Through satellite studies, the moment of inertia of Earth has been deduced to be 8.02×10^{37}kg-m^2. The Lunar mean radius was deduced to be 1738km by the occultation of stars by the edge of Moon. But by Ranger Impacts it has been improved to be (1734.8±0.3) km. Density of Moon was deduced to be 3.361±0.002gm/cm^3.

The measurements made by Astronomical Satellites in 1963 gives a more precise set of data about Earth-Moon System.

Conventionally Principle Moment of Inertia around the spin axis of Earth is
$C= (0.4)\ M_E R_E^2 = 97.06\times10^{36}$Kg-$m^2$.

By Astronomical Satellites the value comes out to be $C= (0.33)\ M_E R_E^2 = 80.26\times10^{36}$Kg-$m^2$. This reduction comes out because Earth is not a homogenous spherical mass but a stratified oblate, ellipsoid with highest density of mass at the core and lightest density of mass at the crust.

Secondly the rock samples brought from our Moon during Apollo 11 to Apollo 17 Mission and during Luna 16 and Luna 20 Mission conclusively prove that Earth and Moon had been formed from the disc of accretion about 4.53 Gya but they were never a single body i.e. Moon's composition is different from that of Earth [19,20]. The Age of Moon has been found incorrect by recent findings [21,22]. The new age is around 4.467Gya. This has been corroborated by Richard Carlson in his paper "Age of the Lunar Crust: Implications for the time of Moon Formation" presented at "Origins of the Moon" Royal Society Meeting on 23-24th September 2013 organized by David Stevenson and Alex Halliday. His estimate puts the Giant Impact occurrence on Proto Earth around 4.4 to 4.45by ago.

There were three competing hypotheses about the origin of our Moon:

- Fission Model put forward by George Howard [5];
- Capture Model;
- Double Planet Theory or Co-formation Theory.

None of these theories were consistent with the facts that emerged after extensive study of the Lunar Samples, after interpreting the data received from the network of seismometers set up on the surface of our Moon and after spectroscopic studies of Moon's crust. Finally, in 1984 at the International Conference held at Kona, Hawaii, GIANT IMPACT HYPOTHESIS was accepted as the most consistent hypothesis regarding Moon's Origin [11].

According to this hypothesis a Supernova Explosion occurred in the neighborhood of our Solar System. The shock waves from this explosion caused a neighboring Giant Interstellar Cloud of gas and dust to go into spin mode. The rapid spinning of the Giant Cloud flattened it into a pancake called the disc of accretion or the primordial Solar Nebula around 4.568by ago.

The nucleus of this Solar Nebula gravitationally collapsed into a ball of Nuclear Fusion Furnace called our Sun [23]. This gave birth to the protoplanetary disk of gas and dust.

According to the Current Model of planetary formation, the disc of accretion would form around any forming star [24-28]. This disc of accretion is not unique to our Solar System. In our case disc was 50 AU where 1 AU (astronomical units) is the distance between Earth and our Sun. It is postulated that at 4.568Gya the Solar Nebula was formed. By 4.567Gya there were dust particles embedded in hydrogen gas. Through gentle collisions these dust particles aggregated into larger particles of centimeter or more size. These larger particles either through collision-agglomeration or through gravitational instability coalesced together to form kilometer sized planetesimals. Meteorites are the residues of these planetesimals. This process was completed in one million year by 4.567Gya. A dense swarm of planetesimals in near circular, low-inclination orbits is gravitationally unstable on a short time scale. In less than one more million year much larger bodies of 10 km size are formed through collision and accretion. These larger bodies are planetary embryos and are Moon- to Mars- sized. From this point on ward the current model is unsure of the series of events which led to the evolution of our present Solar System.

In spite of the ambiguity there are a few points where there is a wide consensus:

- Formation of Gas Giant Jupiter preceded the formation of all planets in our Solar System;
- For next 5 to 30 million years there was enough hydrogen to give birth to the Gas Giants. After 5 to 30 million years the gas-residual dust disc should get dissipated by photoevaporation and Robertson-Poynting drag;
- This means by next 5 to 30 million years Jupiter, Saturn, Neptune and Uranus formation should be complete;
- Further Jupiter and Saturn migrated from inside to their present orbit which caused 1:2 Mean-Motion-Resonance crossing at about 300My after the birth of Solar Nebula [http://arXiv.org/abs/0807.5093];
- Jupiter's migration had a significant role in the subsequent formation of terrestrial planets;
- Terrestrial Planets including Earth were not formed through gradual accretion by the planetary embryos but through a series of infrequent and highly traumatic impacts separated by periods of cooling and healing;
- The last such event in case of Planet Earth was the lunar forming Giant Impact (with the finding of Zhang et.al. (2012) this becomes uncertain);
- The latest isotopic evidence place this event at 4.467Gya or at 4.4Gya;
- It is also now accepted that 1:2 MMR crossing was responsible for Late Heavy Bombardment Era occurring from 4.0Gya to 3.8Gya [29];

Pluto is a captured body which was not formed by normal process of accretion or by a normal planetary formation process.

According to the present studies of meteorites, spinning Solar Nebula was born 4.567 Gya and Earth formation was complete by 4.467 Gya in a time span of 100 million years [21,22].

About this time Earth experienced a glancing angle collision from a Mars-sized planetary embryo. Earth acquired an angle of Obliquity which presently is Φ 23.5° and a rapid spin of 5 hours per revolution. The Impact generated circumterrestrial disc of debris accreted within Roche's zone to form our Moon [30,31]. Giant Impact involved a Mars size mass planetary embryo (10% of Earth's mass) and 90% of complete Earth. Most of the impact energy was dissipated as heat but the total angular momentum has been conserved till this day. The core of the projectile merged with

the core of the proto Earth. Some of the Earth's atmosphere got blown off. The molten mantle froze before it could differentiate. After the impact a circumterrestrial disk of debris was generated. There was a rapid exchange of material between the molten Earth and vaporized disk. This led to similarity in Oxygen isotope in Earth and Moon. Tungsten and possibly Silicon isotope also point to this kind of exchange and achieving an equilibrium in the aftermath of Impact.

Oxygen isotopic compositions have been found identical in terrestrial samples and lunar samples. This is inconsistent with numerical models estimating that more than 40% of the Moon was derived from Theia responsible for the Giant Impact, the favoured scenario for the Moon formation till now [32-34]. It has been found that $^{50}Ti/^{47}Ti$ ratio in Moon is identical to that of Earth within 4 parts per million [16]. The isotopic homogeneity of this highly refractory element suggests that lunar material was derived from proto-Earth mantle. This gives support to Moon being Earth's daughter. But the simulation by Cuk and Stewart (2012) reconciles the Giant Impact with fission hypothesis put forward by George Howard Darwin.

Earth-Moon System Analysis based on Seismological Consideration

The technique first adopted by George Howard Darwin (Darwin 1879,1880), by Genstenkorn (1955), by Macdonald (1964) and Kaula (1964) was that of setting up of dynamical equations and integrating back in time. Rubincam (1975) showed that Moon does have an equatorial origin therefore it could have formed by fission or by accretion. Touma et al (1998) has worked out the eviction resonance and secular inclination-eccentricity resonance that excites 10 degree inclination in the remote past. Williams et al (1998) have worked out the obliquity-oblateness feedback process and tried to rationalize the present day obliquity of Earth at 23.5° and lunar orbital plane inclination at 5°. Ward et.al.(2000) have shown that substantial lunar orbital inclination of about 15° in the remote past could be caused as a natural result of its formation from an impact generated disk.

Touma et.al. (1994) do the Hamiltonian reformulation of the multiply averaged secular theory of Goldreich (1966) and use this to examine various tidal models. They make less severe approximations by including second order effects. Touma uses symplectic integration scheme for studying rotational and orbital motion of extended bodies in the planetary n-body problem.

Cameron, the progenitor of Giant Impact theory, was the first person to do simulation of the impact process. Along with and have published their simulation results in ICARUS [44-47]. Canup and Esposito published their simulation results also in ICARUS (1996). Simulation work was also done by [47,48]. A new technique known as Smooth Particle Hydrodynamics (SPH) has been developed and utilized for impact simulation by [10,49]. The most recent simulation yields iron-poor Moon as well as the present mass and angular momentum of the Earth- Moon system [49]. This class of impacts involves a smaller and thus more likely impacting object than previously considered viable, and suggests that Moon formed near the very end of Earth's accretion. The latest works on the Dynamical History of E-M System have been done by [50-52]. But to date all the works suffer the pitfall of too short or too long an evolutionary span of time from the inception to the present time.

Earth-Moon System analysis based on Kinematic consideration

On the basis of the Lunar Laser Ranging Data released by NASA on the Silver Jubilee Celebration of Man's landing on Moon on 21st July 1969-1994, Gravitational Sling-Shot model of Earth-Moon System was discovered (http://arXiv.org/abs/0805.0100) which satisfactorily gave the analytical basis of the lengthening of day curve and the analytical analysis of the delta-T curve (Chapter 2, Author's D.Sc. Thesis) [53-58]. Gravitational Sling Shot Model gives two geo-synchronous orbits for Moon: inner and outer geo-synchronous orbits namely aG1 and aG2. Further analysis shows that inner geo-sync orbit is unstable equilibrium orbit with an energy maxima whereas outer geo-sync orbit is stable equilibrium with energy minima. In 2016 Matija Cuk and his colleagues put forward the 'Fits and Bound Model' of Earth Moon system. This model finally solved the long standing problem of perfect match between Observed Length of Day Curve and Theoretical Length of Day Curve over last 1.2Gy from the present with implications for Early Warning System for impending Earth-quakes and sudden Volcanic Eruptions [31].

The gravitational sling shot was applied to Phobos, Deimos and Charon, the moons of Mars and Pluto respectively, and satisfactorily explained their orbital configuration [59] (http://arXiv.org/abs/0805.1545).

In a similar work by, the results obtained are as follows:
"Analytical consideration shows that if the contemporary lunar orbit were equatorial the evolution would develop from an unstable geosynchronous orbit of the period 4.42h (in the past) to a stable geosynchronous orbit of the period 44.8 days (in the future) [52]. It is also demonstrated that at the contemporary epoch the orbital plane of the fictitious equatorial moon would be unstable in the Lyapunov's sense, being asymptotically stable at the earlier stages of the evolution."In Table 1, a comparison of results of Author's analysis and those of is given [52].

Table 1: Comparative Study of the Results Obtained by and Sharma (Personal Communication)

	aG1/R_{Earth}	aG2/R_{Earth}	Orbital period at aG1	Orbital period at aG1
Krasinsky analysis	2.15	83.8	4.42h	44.8days
BKS analysis	2.29	86.65	4.8596h~5h	47.0739days
George Howard Darwin analysis	Not available	90.4	Not available	47days

Author's kinematic analysis of Earth-Moon System gives the correct evolutionary time span of 4.467Gyrs, the present Age of Moon [15,31,52].

There is no empiricism involved in arriving at the best fit value of the various parameters of the Planet-Satellite system. There is a general Primary-centric Framework in which any two-body system - it may be Planet-Satellite System, Planet-Planet Hosting Star System or Brown Dwarf Binary System may fit [60,61].

The Birth of the Architectural Design Rules based on the New Perspective (2004)

In 2004, the Author presented a New Perspective on the Birth and Evolution of our Solar System at 35th COSPAR Scientific Assembly in Paris, France [9]. The Author further applied this New Perspective to a large number of exo-solar systems and exo-planets [60,61].

The Architectural Design Rules based on the New Perspective [9,61] can be summed up as follows:

The New Perspective says that in any solar or exo-solar system or in any binary system

- There are two Clarke's Orbits (inner Clarke orbit aG1 and outer Clarke orbit aG2);
- Here Clarke's orbit is defined as the orbit where the two bodies are tidally interlocked with each other, orbit is circularized and components are synchronized meaning by no tidal dissipation is taking place and spin period of the primary = orbital period of the binary = spin period of the secondary. This I will refer to as triple synchrony state;
- Region beyond aG2 is a forbidden zone for the secondary. The secondary can never enter the forbidden zone of orbits. If it does it will be deflected back;
- This gives a criteria for determining gravitationally bound binary. If the secondary lies at or within outer Clarke's orbit then it is a gravitationally bound binary else the two bodies are freely floating in space;
- Inner Clarke's Orbit is free energy maxima hence it is an orbit of unstable equilibrium (My manuscript on Circumbinary Planets) [52]. Slightest perturbative force causes the secondary to tumble short or long of aG1;
- If the secondary tumbles short of aG1 then it is in sub-synchronous orbit and the secondary gets trapped in gravitationally runaway collapsing spiral orbit. The secondary is destined to either coalesce with the central body or get tidally disrupted as it enters Roche's Zone [10]. Hence this collapsing spiral orbit is also referred to as death spiral;
- If the secondary tumbles long of aG1 it experiences an impulsive torque which I call gravitational sling-shot which imparts a large amount of rotational energy to the secondary. The secondary is launched on an expanding super-synchronous spiral orbit where it coasts on its own by virtue of its initial energy boost towards the outer Clarke's orbit;
- Once in outer Clarke's orbit it may remain stay put in that orbit or by third body perturbation it may be deflected back on a collapsing spiral orbit. The outer Clarke's orbit is energy minima and hence an orbit of stable equilibrium (Krasinsky 2002, My Manuscript on Circum-binary Planets);
- Only in inner and outer Clarke's orbits the system is in truly Keplerian State that is the centrifugal force is exactly balanced by the centripetal force. In any other orbits there is a wee bit imbalance hence the secondary is in migratory phase;
- When the secondary to primary mass ratio 'q' is less than 10^{-3} , time constant of evolution $\tau = (a_{G2} - a_{G1})/V_{max}$, where Vmax is the maximum outward radial velocity acquired by the secondary during gravitational sling shot phase, is of the order of Gy and evolution factor is a low fraction [€ = $(a - a_{G1})/(a_{G2} - a_{G1})$] .
- If the mass ratio is 10-2 then time constant is My and evolution factor is in 0.5 neighborhood. This will also depend on the age of the system.
- When the mass ratio is in the range of 2×10^{-1} to Unity then the time constant is in years/months/days and evolution factor is near unity no matter what the age is but not unity [9,59-61].
- For $0.2 \leq q \leq 1$, hydro-dynamic instability leads to the formation of the two components and for $q < 0.2$, core-accretion process is the formative process for the secondary,
- Scoring a perfect score of UNITY evolution factor (€) will depend upon tidal circularization time-scale and tidal synchronization time scale. If the two time scales are within the observed age of the binary then the system will fall in triple synchrony state and the binary will score an unity evolution factor otherwise there will always be an offset from Unity evolution factor €.
- What this implies is that if the mass ratio is a large fraction larger than 0.2 then the secondary immediately falls into the near outer Clark's orbit no matter what the age of the system is and if mass ratio is low (less than 0.2) then the secondary gradually evolves from inner to outer Clark's orbit and the system has a evolutionary history and the present configuration will be a function of the time constant of evolution as well as the age of the system.
- If the secondary is infinitesimal mass fraction as the man-made satellite is then it remains in inner Clarke's orbit and it has no evolutionary history [In case of man-made satellites it is 36,000Km above the equator in equatorial plane].
- For strongly relativistic binaries such as Double Neutron Star Binaries, the near outer Clarke's configuration is achieved on month/year time scale but final triple synchrony is never achieved due to gravitational radiation induced spiral-in hence a finite offset with respect to unity evolution factor will always remain no matter what the age is. But this offset will be related to the strength of the relativistic system, measured by the mean rate of advancement of the periastron.
- A binary system is amenable to theoretical analysis only if the spin-orbit-globe parameters are correctly and accurately known. Any mistake in the spin-orbit-globe parameters will make the system untenable to mathematical analysis.

High mass ratio binary falling in near outer Clarke's Orbit had been identified by [62,63]. The Author quotes Zahn in the following paragraph:

"Eventually the Binary may settle in its state of minimum kinetic energy, in which the orbit is circular, rotation of both stars is synchronized with the orbital motion and the spin axis are perpendicular to the orbital plane. Whether the system actually reaches this state is determined by the strength of tidal interaction, thus by the separation of the two components, equivalently the orbital period. But it also depends on the efficiency of the physical process which are responsible for the dissipation of the kinetic energy."

Architectural Layout of Binary Systems in Primary-Centric framework as a Function of Mass Ratios

A paper titled "Iapetus hypothetical sub-satellite revisited and it reveals celestial body formation process in the primary-centric framework" was presented at 39th COSPAR Scientific Assembly 2012, Mysore, India [B0.3-0011-12] and its revised manuscript has been published [64]. In that paper the architectural layout of binaries for different mass ratios were studied and the following results were obtained.

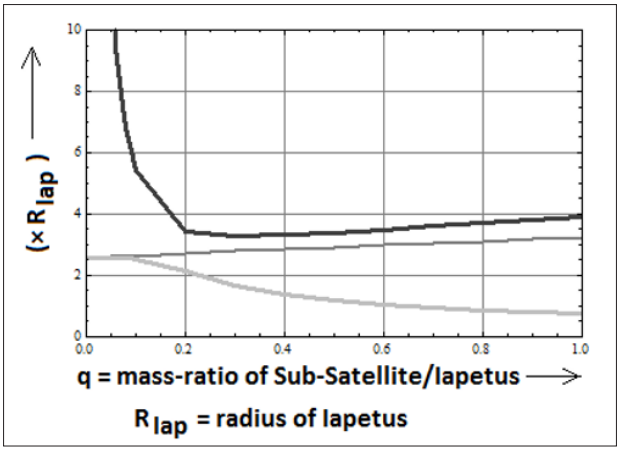

Figure 1: Plot of a_{synSS} ($\times R_{Iap}$) [Thin-Gray], aG1 ($\times R_{Iap}$) [Thick-Gray] and a_{G2} ($\times R_{Iap}$) [Thick-Black] as a function of 'q'. [BP3.eps]

In Figure 1, Thin-Gray line gives the plot of triple synchrony orbit from classical Keplerian Formalism of Sub-Satellite with respect to 'q'. Thick-Gray line gives the plot of inner Clarke's Orbit and Thick-Black line gives the plot of outer Clarke's Orbit with respect to 'q' respectively. Inner and Outer Clarke's Orbits are obtained only from Primary-centric formalism. Classical Keplerian Formalism never yields two triple synchrony orbits. It yields only one orbit which is designated as a_{synSS}.

Inspection of Figure 1, tells us that at infinitesimal values of 'q', a_{synSS} is the same as aG1 and only inner Clarke's Orbit is perceptible. But at larger mass ratios the two (classical and primary-centric formalism) rapidly diverge. The Author analysis till now has confirmed that aG1 is the correct formalism for predicting the inner triple synchrony orbit in a binary system at $q < 0.2$.

At mass ratios greater than 0.2, a_{G1} is physically untenable and only aG2 is perceptible. Outer Triple Synchrony Orbit tends to converge but never actually converges to the classical formalism but remains off-setted right till the limit of q=1. Here again only outer Clarke's Orbit is perceptible. The actual Star pairs satisfy the Primary-centric formalism and not the classical formalism.

So Primary-centric World View, though satisfies the correspondence principle at $q \sim 0$, is a theory in its own right.

Till date there exists no formalism for two triple synchrony orbits in Classical Keplerian Mechanics in the mass ratio range 0.001 to 1.

For mass ratio less than 0.0001, binaries remain in inner Clarke's Configuration in a stable state which is predicted by Classical Keplerian Formalism also. This we see in Geosynchronous man-made satellites at 36,000Km above the equator in equatorial plane.

At mass ratios greater than 0.2 right up to unity, non-relativistic star pairs remain in outer Clarke's Configuration stably and its magnitude is more than Keplerian prediction as seen in Figure 1 and as seen in subsequent analysis.

For mass ratios $0.0001 < q < 0.2$, Outer Clarkes configuration is the only stable orbit. Secondary originates at a_{G1} and the pair migrates out of that configuration. If it is at $a > a_{G1}$ the pair spirals out with a time constant of evolution and if $a < a_{G1}$ then the pair spirals-in on a collision course again with a characteristic time constant of evolution.

Time Constant of Evolution (τ) is in inverse proportion of some power of mass ratio. For q = 0.0001 and less, tidal interaction is the least and 'τ' is Gy. As q increases tidal interaction increases, time-constant decreases from Gy to My to kY to years. Between 0.2 to 1, tidal interaction is the strongest and a solar nebula falls into outer Clarke's Configuration by hydro-dynamic instability within months/years.

Primary-centric formalism has an analogue in Bohr's Model of Atom. Just as electrons have only stationary orbits or non-radiative orbits as permissible orbits. In exactly the same way, binaries have triple synchrony lock-in orbits as the permissible orbits which are completely non-dissipative and conservative.

Application of Architectural Design Rules to Keplerian Binaries namely White Dwarf and Low Mass M Dwarf Star in precataclysmic binary NN Serpentis and RW Lacertae (GSC 03629-00740)

Keplerian binaries are the binaries where mass has been calculated by the Doppler shift in the spectral lines due to the radial velocities of the two components [65,66]. Here there is no detectable advancement of the periastron hence it has no gravitational radiation and such binaries are classified as a Keplerian Binary or non-relativistic Binary.

According to the Architectural Design Rules, in a star binary or star-white dwarf binary the system should settle down immediately to near-outer Clarke's Orbit with the binary system settling in triple synchrony state within tidal locking time scale (t_{lock}). So if the t_{lock} is within the age of the binary, the star-binary or star-WD binary should settle in triple synchrony state
Hence $P_{spin\_WD} = P_{spin\_sec} = P_b$.

In case of young binary system this will not be the case as is evident from Table 2.

Table 2: Spin Period and Orbital Periods of Young Star-WD binary pairs

	Age (My)	P_{spin_WD}	P_{spin_sec}	P_b	Ref
V471 Tau	10	555s	45000s	45000s	1
EC13471-1258	young	120s	13020s	13020s	2

As is evident from Table 2, in V471 Tau and EC13471-1258 the secondary is tidally locked and hence has a synchronous motion but it has not had enough time for lock-in with the Primary [67,68]. Therefore, Primary Spin Period is less than that of the Secondary. Secondary is not tidally inter-locked with the Primary.

In case of 'star-white_dwarf' systems which are old, triple synchrony is possible by tidal inter-locking within its life time. In case of NN-Serpentis, the mass of WD is close to a mean White Dwarf mass and the initial-final mass relation is flat in this region. This means a large range of progenitor masses are possible for the WD hence a large uncertainty exists in its age.

Tidal Locking in Main Sequence is well studied and it has the following formulae [69,70]:

$$t_{lock} = \frac{16\rho\omega a^6 Q}{45 G m_p^2 k_2} \qquad 2$$

Where ρ = density of the secondary; ω= initial spin rate of the secondary; a= semi-major axis of the orbit; Q = dissipation factor of the secondary body; G = Gravitational Constant; m_p = mass of the primary; k_2 = tidal second order Love Number of the secondary;

For terrestrial planets and satellites: Q = 10 to 500;
For Jovian Planets: $Q = 6\times10^4$;
The typical values taken for NN Serpentis WD are:
$\rho = 80.42\times10^6 Kg/m^3$; ω= (2π/1123) radians/sec; $a= 0.934R_0$;
Q = dissipation factor of the WD parameterizes the tidal dissipation rate which is not at all constrained if P_{orb}' is not known which in this case is not known = 2.5×10^5 [71].
$k_2 = 0.01$ [71];
Substituting the parameter values in Eq. 2 we get:
$T_{lock} = 2.38Gy$.

Since the age in this case is a free parameter we can assume NN Serpentis to be old enough for tidal lock-in. In this case, the best fit estimate of White Dwarf Spin is also synchronous. So, we can assume triple synchrony state hence $P_{spin\_sec} = P_b = P_{spin\_WD}$ =11232 s

Table 3: Globe-Orbit Parameter of NN Serpentis

parameter	Rel.magnitude	Abs. magnitude
a(semi-major axis)	0.934±0.009R_O	6.49597×10^8m±6.2595×10^6m
R_1(rad.ofWD)	0.0211±0.0002R_O	14.67505×10^6m
R_2(Rad. of M Dwarf)	0.149±0.002R_O	1.036295×10^8m
M_1(mass of WD)	0.535±0.0121M_O	1.06465×10^{30}Kg
M_2(mass of M Dwarf)	0.111±0.004M_O	2.2089×10^{29}Kg
$P_{orb} = P_{spin1} = P_{spin2}$	0.13days	11232s

For radii, masses and orbital period we take the nominal value but for semi-major axis we take $a=6.441298528815612\times10^8$m which is a optimum fit parameter within the margin of error of the semi-major axis as given in the Table 3 [65].
Total angular Momentum of the binary:

$$J_T = 0.4M_1R_1^2 \times \left(\frac{2\pi}{P_{spin1}}\right) + 0.4M_2R_2^2 \times \left(\frac{2\pi}{P_{spin2}}\right) + \frac{M_2}{1+\frac{M_2}{M_1}}a^2 \times \left(\frac{2\pi}{P_{orbit}}\right) \quad 3$$

Substituting the values of the parameters from Table 3 in Eq 2. We get:
$J_T = 4.3014808254581605\times10^{43}$ Kg-m^2-sec^{-1};
Similarly, the magnitudes of the various parameters from Table 3 are substituted in the following equations:
$B = \sqrt{[G(M_1+M_2)]} = 9.259170384720997\times10^9 m^{3/2}/s$ 4
$CO = 0.4M_1R_1^2 = 9.165654060541976\times10^{43}$ Kg-m^2 5
$E = J_T/(BC_0) = 5.06853504593348\times10^{-11} m^{-3/2}$ 6
$F = (M_2/(1+M_2/M_1))\times(1/C_0) = 1.994671076191769\times10^{-15} m^{-2}$ 7
The observed (ω/Ω) = observed (P_{orbit}/P_{spin1}) = 1

From spin/orbital equation:
Calculated value of $(\omega/\Omega) = E\times a^{3/2} - F\times a^2 = 1$;
We find that the calculated and observed value of the spin/orbital ratio are the same and at unity. As we have already predicted that for mass ratio q>0.2, the system on a very short time scale of months/year falls in outer Clarke's configuration and given enough time it settles down in the triple synchrony state at the outer Clarkes Orbit configuration.

The roots of the spin to orbital equation:
$E\times a^{3/2} - F\times a^2 = 1$ are
aG1 =7.89476×10^6m and aG2=$6.441298528815612\times10^8$m
whereas a = $6.441298528815612\times10^8$m

Here the evolution factor €= Unity and the M Dwarf and White Dwarf are inter- locked at the triple synchrony state at outer Clarke's Orbit with zero tidal dissipation. The permanent oblately deformed shape of the two components with perfect alignment of the two major axis of the ellipsoidal components rotating around the barycenter ensures a non-dissipative and hence a stable outer Clarke's configuration. There is absolutely no periodic stretching and squeezing of the two components. During the tidal lock-in phase the two components got permanently stretched into ellipsoidal oblong components and eventually the two got aligned along the major axis. This is the mutually inter-locked configuration.
Therefore, PCB NN Serpentis obeys the Architectural Design Rules.

Architectural Design Rules applied to RW Lacertae (GSC 03629-00740)
RW Lac is a detached, eccentric, EA-type, 10.37days orbital period, double-lined eclipsing binary star belonging to the class of Keplerian binaries [66]. The orbits are slightly eccentric indicating that the tidal circularization is not complete during its existence of 11Gy as a binary. The spectral line-widths give observed rotational velocities which indicate triple synchrony state. The components of the binary are old, some-what metal deficient, low mass, main sequence stars with an age of 11Gy. The tidal locking time of the two components are 2.92Gy and 3.18Gy hence the synchronization time is well within its observed Age. Therefore, its evolution factor (€) makes a perfect score of unity as shown in SOM Appendix A.

Relativistic Binaries
Stars have three destinies: White Dwarf, Neutron Stars and Black holes. Stars with mass less than $1.4M_0$ are destined to end up as White Dwarf where electron degenerate pressure balances the gravitational collapse. Stars with mass between $1.4M_0$ and $3M_0$ end up as Neutron Stars (NS) where neutron degeneracy pressure balances the gravitational collapse. Stars with mass greater than $3M_0$ end up as Black Hole (BH). According to general theory of relativity such a star as BH is in a state of free fall and all the matter is entombed in a singularity. Inside time passes very slowly (time dilation) and the star is collapsing at relativistic speeds but from outside it is at equilibrium defined by event horizon. Event horizon is defined as a sphere with Schwarzschild Radius [72].

$$r_s(Schwarzchild\ radius) = \frac{2GM_{BH}}{c^2} \quad 8$$

Where $G = 6.673\times10^{-11} m^3Kg^{-1}sec^{-2}$; c = velocity of light; M_{BH}= mass of the central black-hole = $10^M \times M_O$;

Table 4: The properties of White Dwarf, Neutron Star and Black Hole

Type of remnant	Matter density	Mass	Diameter
White Dwarf	$10^9 Kg/m^3$	Less than 1.4M○	12000km
Neutron Star	10^{17}Kg/m^3(density of the nucleus)	1.4M○ to 3M○	20km
Black Hole	singularity	Greater than3M○	Event horizon

Neutron Stars and Black Holes are the densest manifestation of massive objects. These have the largest surface gravitational potential [73,74].

$$Surface\ gravity = Compactness = \frac{GM}{c^2R}\ (dimensionless) \quad 9$$

Compactness or relativistic surface gravitational potential of Main Sequence Star, White Dwarf, Neutron Star and Black Hole progressively increases as shown in Table 5.

Table 5: Relativistic Surface Gravitational Potential (or Compactness) of Main Sequence Star, White Dwarf, Neutron Star and Black Hole

	Compactness	Mass(Kg)	Radius(m)	ρ(Kg/m^3)
M Dwarf in NN-Serpentis	1.58×10^{-6}	$0.111M_0$	1.0363×10^8m	47384
White Dwarf (NN-Serpentis)	5.39×10^{-5}	$0.535M_0$	14.675×10^6m	80.42×10^6
Neutron Star (Hulse-Taylor)	0.212	$1.4411M_0$	10Km	7×10^{17}
Black Hole	0.5	1×10^5M_0	2.95×10^8m(event horizon)	1.85×10^9

The surface gravitational potential clearly classifies NS, BH and their binaries as astrophysical objects which require relativistic theory of gravity for their description. In the region of Sun-Mercury we experience weak field regions of relativistic gravity which is responsible for the miniscule advancement of periastron by 43 arc second in a century. In Double Neutron Star Binary (DNSB), Black Hole Binary or in NS-BH Binary we are dealing with strong field region of relativistic gravity. Combinations of NS and BH comprise the relativistic binaries. Strength of the relativistic binary is determined by the rate of advance of the long axis of the elliptical orbit around the barycenter. This is also known as the rate of advancement of the periastron or is also referred to as apsidal motion. We will be investigating 6 Double Neutron Star Binaries (DNSB) namely: J1811-1736, J1518+4904, B1534+12, B1913+16, B2127+11C and J0737-3039. In Table 6, these DNSB and their respective apsidal motions are tabulated.

Just for creating the distinction between the non-relativistic and relativistic binaries we have included the apsidal motion of Mercury with respect to the Sun.

Table 6: Comparative Study of the Apsidal Motion and the Offset from Unity Evolution Factor for Six Pulsar Binary Systems

Name of PSR	Apsidal motion(ω')	Offset	(i)°	Reference
J0737-3039	16.88°/y	8.5×10^{-3}%	87°	App.A
B2127+11C	4.4636°/y	4.0×10^{-3}%	49.66°	App.C
B1913+16	4.226°/y	2.14×10^{-3}%	47.233	Text
B1534+12†	1.76°/y	3×10^{-3}%	77.34°	App.B
J1518+4904	0.0111°/y	1×10^{-3}%	45°	App.D
J1811-1736	0.009°/y	0.312×10^{-3}%	48.6°	App.E
Mercury-Sun	43 arcsec per century			Tiec et.al [2011]

This answer is suspect as the system parameters of B1534+12 have a low confidence range(Stairs 2003). Careful analysis of the timing data for B1534+12 has revealed the presence of unmodeled orbital effects of unknown origin. (Wolszcyan 1997). This could be the reason for low confidence range for the system parameters.

As can be seen from Table 6, Mercury-Sun is in the weak field regime of relativistic gravity hence apsidal motion is negligible whereas J0737-3039 has the largest apsidal motion in the sample of DNSB chosen. If we took BH binaries the apsidal motion would be still more rapid. Mercury takes 12 million orbital periods to make a periastron advance of 360°, J0737-3039 takes 76181 orbital periods to make a periastron advance of 360° and BH pair takes only two orbital periods to make 360° advance [75].

From Table 6, it is also clear that as the strength of relativistic DNSB increases the offset with respect to the Unity Evolution Factor increases. The reasons we will discuss in the succeeding sections.

A NS acts like a light house sweeping across the space and if we happen to fall in its line of sight we detect a NS and if the light repetition period is periodic then we have an isolated NS and if the time-of-arrival (t.o.a.) has an irregularity then we have detected a DNSB. This is what happened when the celebrated Hulse Taylor pair was discovered in 1974 at Arecibo Observatory, Puerto Rico.

Single NS act as the best time keepers in the Universe even better than the atomic clocks that we have on our Earth. One such Cosmic Clock is PSR B1937+21 which was discovered in 1982 by Donald Backer Group at University of California, Berkeley [78]. This was a special class of Spun-up or recycled pulsars which are extremely stable rotators. PSR B 1937+21 has P_S = 1.557708ms. It exceeds fractional frequency stability of 10-14 on a time scale of several years [79].

Because of the light house characteristics, NS was named a Pulsar. It mostly emitted Radio Waves hence it was known as Radio Pulsar but it could as well emit optical waves, X-rays and Gamma Rays depending on its physical environment.

Pulsars present an extreme stellar environment, with matter at nuclear densities, magnetic fields of 10^8 G to nearly 10^{14} G, and spin periods ranging from 1.5 ms to 8.5 s. The Pulsar has a dipole magnet which is not aligned with its spin axis and powerful cone of synchrotron radiation are coming out of the two poles of the magnet [43,80,81]. Because of the mis-alignment, this cone sweeps the space surrounding the spinning Pulsar on the broad-side (near-equatorial side). Larger will be the mis-alignment larger will be the broad-side illumination. If we happen to be in its line-of-sight we record periodic arrival of pulses.

By precision recording of the time of arrival of the pulses we can deduce 18 parameters. Pulsar Spin, 4 Astrometric Parameters, 5 Keplerian Parameters(projected semi-major axis x_p , eccentricity e , orbital period P_b, longitude of periastron ω and epoch of periastron T_0) and 8 Post-Keplerian parameters (x_p' , e' , P_b', ω', Einstein parameter γ and range 'r' and shape 's' of Shapiro Delay plus Orbital Shape Correction δ_0). 5 Keplerian parameters, and 2 PK parameters are sufficient to constrain the masses of the two pulsars. If more than 2 PK parameters are available then we over determine the equations and this provides a test for strong-field relativistic gravitational theories. The high timing precision made possible by the narrow pulses of this pulsar, promise to make this system an excellent 'laboratory' for the investigation of relativistic astrophysics.

In the System Parameters Tables, we have only the projected semi-major axis (x) and for the Primary-centric analysis we require the actual semi-major axis (a). Therefore, the precise knowledge of Sin(i) is necessary. Either we measure the shape of Shapiro Delay or we calculate Sin(i) by the following formula [82]:

$$\sin i = G^{-\frac{1}{3}} c \left(\frac{a_P \sin i}{M_C}\right)\left(\frac{P_b}{2\pi}\right)^{-\frac{2}{3}} (M_P + M_C)^{\frac{2}{3}} \qquad 10$$

The Shapiro Delay requires an edge-on view of the system which may not be the case or favorable orientation can become unfavorable due to Geodetic Precession [83].

General Relativistic Gravitomagnetic spin-orbit coupling causes geodetic precession [83,84]. Asymmetry in SN Explosion that created the companion of Hulse-Taylor Pair caused the misalignment of Jspin and Jorb, the spin angular moment and orbital angular momentum. This leads to the precession of spin angular momentum vector around the orbital angular momentum vector of the system. This precession alters the pulse emission beam with time with respect to the observer leading to change in the observed pulse morphology. Detailed measurement of the pulse structure of Hulse-Taylor Pair have resulted in detection of a systematic, slow changes in the average pulse morphology which can be explained in terms of geodetic spin precession. In earlier datasets in Hulse-Taylor Pair, it was possible to solve for the two parameters of the Shapiro gravitational delay, r and s, and they were marginally constraint [85,86]. As the orbit has processed, however, the geometry has become less favorable for measuring this phenomenon. Continuing orbital precession is now causing the Shapiro signature to begin to grow again.

General Relativity predicts geodetic precession periods of 75 years for A component and 71 years for B component in DNSB PSR J0737-3039.This is the shortest precession period discovered till date [83].

The range of NS masses observed in binary systems is much narrower than that is permissible between 0.1 to 3 ($\times M_0$) resulting from the general relativistic Equation Of State of a NS (Beyn & Pethick, 1979, Ann. Rev. A & A, 24,1986,537).

The observed masses agree with a typical value of $1.3M_0$ obtained under the assumption that NS is a product of the collapse of stellar masses that exceeded Chandrashekhar Limit.

Physics and Observational Properties of Pulsars

We have seen that Neutron Star is a pulsar and NS is a result of stellar collapse [87,88].

Stellar Collapse takes place due to the following reasons:

- There is a failure of central energy supply;
- Lack of radiation pressure causes gravitational collapse;
- The nature of the gravitational collapse depends on core mass.

Table 7: Core Mass determines the Nature of Gravitational Collapse

Core Mass	Type of Star	Type of SN explosion
1.9 to $2.5M_0$	Neutron Star	Type II(150d_short lived burst of energy peaking at 50d)
$<1.9M_0$	No remnant	Type Ia(delayed peak and energy burst tails out to 300d)
$>2.5M_0$	Black Hole	Type II(150d_short lived burst of energy peaking at 50d)

Core Collapse causes neutrino emission. Core Bounce causes explosion and there are few hours delay between neutrino and photons, neutrinos arriving several hours earlier. From Table 7 we conclude that NS is the product of Type II Super-nova explosion.

The pulsars have high spin rate due to gravitational collapse, the spin period can vary from 1.5ms ~ 11 s. But the original pulsar is always in seconds period range. It is these second period range old pulsar which are recycled and reborn in a binary as a milli second pulsar (MSP). So MSPs are rejuvenated old pulsars.

It has a powerful dipole magnet with a surface magnetic field as high as 10^{15}G and as low as 10^{8}G. Because of the strong magnetic field and due to high spin rate, Pulsar are efficient dynamos generating electric fields 10^{12}V/cm or more near its surface. Charged particles are accelerated to ultra relativistic energies in these large electric fields leading to electron-positron production avalanche and ultimately to the generation of synchrotron radiation from the polar caps. Due to magnetic dipole radiation and due to charged particle winds all pulsar spin-down. From the spin-down rate, the characteristic age which is the upper limit of its real age and the residual magnetic field can be determined as shown in Table 8.

Table 8: Typical Characteristic Age (τC) and Residual Magnetic Field after Spin-down

	P_S	P_S'	$\tau C = P_S/(2P_S')$	$BS=3.2\times10^{19}\sqrt{(P_S P_S')}$
PSR	1 s	10^{-15}s/s	15.8My	10^{12}G
MSP	<20ms	5×10^{-20}	6.33Gy	10^{9}G

Looking at the Table 8 it is obvious that fast spinning MSP have considerable decayed magnetic field.

The re-birth of MSP

Nearly 2/3 of all known MSP are in binaries. Further investigation has showed that the remaining 1/3 were also in binaries but during the re-birth process the companion got destroyed. Hence the progenitor PSR of all MSP were gravitationally bound in a binary.

All MSP or MSP-binary started as Main Sequence star binaries which contain A and B component [89]. Component A explodes into Super Nova explosion to form a NS. NS spins down as a normal pulsar due to emission from polar ends hence it is in luminosity spin down mode for 1My to 10My. Component B comes to the end of MS lifetime and becomes Red Giant (RG). By Roche's overflow from RG to NS the system becomes visible as X-ray binary, NS becomes MSP due to matter and orbital angular momentum transfer to Component A. Magnetic field is dramatically reduced and so is the magnetic braking [90,91]. Hence MSP are recycled old Pulsars. Due to mass transfer there is a spin-up. The end product is a rapidly spinning PSR and it has shed its magnetic field. MSP binaries are best suited for detecting, using and testing effects of relativistic gravity.

A limiting spin period is reached because of equilibrium between the magnetic pressure of the accreting NS and the Ram pressure of infalling matter [89,92]. Hence the fastest MSP has a spin period of 1.5ms. At higher spin rate, the relativistic phenomena of "Gravitational Radiation" sets in. This prevent further spin-up. The extra energy for spin-up just leaks out.

Besides mass transfer from B to A, there is mass loss from the system hence there is sharp reduction in separation and it settles to a very compact system of Helium star and NS. A sufficiently massive helium star will subsequently undergo SN explosion and a young secondary NS is formed. Thus, we get NS pair in eccentric orbit with very different magnetic strength and hence different spin down properties as observed in PSR J0737-3039. 'A' component is typical of a NS but component 'B' is significantly smaller for a NS. The separation is of the order of 900,000Km.

Compact DNSB evolve from HMXB (High Mass X-Ray Binary) after a stage of common envelope evolution and spiral in [93].

The Two Scenarios of MSP Rebirth

PSR J0737-3039, B2127+11C, PSR B1913+16 and B1534+12, are compact binaries. In Period-derivative vs Period Graph there is accretion powered 'spin-up line'. This implies the minimum spin period attainable by accretion from a companion star. This is equivalent to period-magnetic field relation expected after Eddington accretion onto a magnetized NS (Physics Report 203,1) [89].

In compact binaries such as PSR J0737-3039, B2127+11C, PSR B1913+16 and B1534+12observed period and derivative are close to 'spin-up line'.

But J1518+4904 and B2303+46 are wide binaries and are located far from the spin-up line. These have similar evolutionary histories but distinct from the evolutionary histories of the compact binaries.

In compact binaries the evolutionary path is same as described in Section 7.2. At the end of the evolutionary history, we have eccentric orbit with reduced magnetic field strength and rapidly rotating Milli-Second Pulsar (MSP). Much of the magnetosphere of the secondary component is blown away by the wind from the Primary. Spin-down luminosity generates Pulser Wind Nebula (PWN). Though the magnetosphere of the secondary is blown away by the PWN, the secondary continues to work as a Pulsar.

The wide binaries J1518+4904 and B2303+46 under study in this paper have a different evolutionary history. Have suggested that 2nd NS has evolved from a very massive MS star (> 40 to 45 M_0) that expelled its envelope without extracting energy from the orbital system hence spiral-in did not occur [94]. Companion stellar envelope was largely shed of its own accord. J1518+4904 and B2303+46's present day period and its derivative are close to those immediately after spin-up (i.e. after the pulsar formation) far from the spin-up line.

Application of Architectural Design Rules to Hulse-Taylor Binary Pulsar [PSR_B1913+16]

In 1974 Hulse and Taylor were making observations at the largest Radio Telescope at Arecibo, Puerto Rico. Hulse and Taylor had discovered 40 Pulsars. One of them clearly distinguished itself as a binary because of the wobble associated with the visible pulsar. The other pulsar's beacon was not falling in the line of sight and hence was completely invisible. Because of the wobble there was a difference in arrival time of the pulses periodically. From this differential arrival time the masses were accurately determined.

While calculating the masses of the neutron stars, this technique involved the gravitational effect of the two Neutron Stars hence the dark matter was also accounted for. So, no dark matter correction be made through out the analysis.

Hulse and Taylor painstakingly monitored it to see if it was in a collapsing spiral orbit due to gravitational radiation energy losses. In 1982 they reported that stable Keplerian system is indeed gradually collapsing with semi-major axis reducing at the rate of 3.5m/yr and orbital period decreasing at the rate for 0.0000765 seconds per year.1981 onward during 27 years of investigation, 5083 Time of Arrival were measured between 1981 to 2001. These are used for fitting. This model accounts for strong gravity as well as radiative emission. They are predicted to make contact in 300My [95].

The observed orbital decay rate was compared with General Relativity predicted values after making the kinematic corrections for Solar System acceleration and for the Galactic Gravitational Field in which Hulse-Taylor pair resides and an excellent agreement was found between the two [82]. This directly confirms that:

- Relativistic Binaries have a gravitational radiation dissipative mechanism which dominates over the tidal dissipation;
- The gravitational radiation propagates through the space-time fabric at a finite velocity 'c';
- The gravitational radiation has a quadrupolar nature.

For this patient and painstaking observation and their elegant theoretical corroboration by General Theory of Relativity, the duo received the Physics Nobel Prize of 1993.

The account of the discovery, excerpted from the Nobel Foundation website (which also has wonderful illustrations) is given at this link: http://www.nobel.se/physics/laureates/1993/illpres/discovery.html
(Copyright c 2001 The Nobel Foundation)

Table 9: Orbital Parameters for PSR B1913+16

Parameters	Value	Ref
Right Ascension	19h 13m 12.4655s	2
Declination	+16°01'08.189"	2
Distance(d)	21,000ly	2
Orbital Period_P_b (d)	0.322997462727(5)	1
Projected semi-major axis_x_p(l-s)	2.341774(1)	1
Eccentricity_e	0.6171338(4)	1
Longitude of periastron_ω(deg)	226.57518(4)	1
Epoch of periastron_T_0(MJD)	46443.99588317(3)	1
Advance of periastron_ω'(deg.y^{-1})	4.226607(7)	1
Gravitational red shift_γ(ms)	4.294(1)	1
Orbital period derivative$(P_b')_{obs}$($\times10^{-12}$s/s)	-2.4211(14)	1
Rate of decrease of P_{orbit}	0.0000764sec/yr	2
Rate of decrease of 'a'	3.5 m /yr	2
Lifetime to final contact	300My	2

In Mass-mass diagram for the PSR B1913+16 system, using ω' and γ parameters listed in Table 9, the pulsar and companion masses are constrained to:
M_1 =1.4408±0.0003M_0 and M_2=1.3876±0.0003M_0 [95,96].

Table 10: Globe-Orbit-Spin Parameter of the two Components of the Pulsar Binary PSR B1913+16 taken for Final Calculation

Parameters	PSR B1913+16_A		PSR B1913+16_B	Ref.
Stellar mass ($\times M_0$)	1.4411		1.3879	1
Projected semi-major axis $x_1 = a_1 Sin(i)/c$ (l-s)	2.3417740		2.43154	1
Sin(i) (inclination in degree) from the formula		0.7341254342138241 (i= 47.233°)		Cal.
$a_A + a_B = a_{AB}$ (actual separation of A & B) (m)		1.9492618530344882 $\times10^9$		Cal.
Spin Period of the component(ms)	59.02999792988 ms		1 sec(assumed)	1
Orbital period(s)		27906.98078		1
Typical value of Radius (R)	10km		10km	2

Here all calculations are carried out considering every system parameter with 16 significant digits in order to get the correspondence between theory and observation [76,95]. Because of unfavorable orientation (oblique view) Shapiro Delay Shape is unavailable

hence Sin(i) is calculated from Eq. (10).
Substituting the system parameters in Eq. (10) we get Sin(i)=0.7341254342138241;
From center of mass concept:

$$x_1 M_1 = x_2 M_2 \qquad 11$$

Therefore the actual separation of the pulsars

$$a_{AB} = a_1 + a_2 = \left[x_1 + \frac{x_1 M_1}{M_2}\right] \times c \times \frac{1}{Sin(i)} \qquad 12$$

Substituting the parameters in Eq.11we get

$$a_{AB} = 1.9492618530344882 \times 10^9 m$$

Calculation of Spin to Orbital angular velocity equation:

Let $R_1 = R_2 = 10$km [76].

In the Table 10, the spin of the secondary Pulsar is not given so I have assumed it to be 1 sec. Hulse-Taylor Pulsar Pair is relatively young.

$$\tau_C = characteristic\ age = \frac{P_{spin}}{2P'_{spin}} = 117.75My \text{ [82]} \qquad 13$$

Hence the secondary has not synchronized with Orbital Period. Infact within the merger time of DNSB, strongly relativistic NS never synchronize [97].

Substituting the numerical values of the orbit, spin and globe parameters in Equation 3, 4, 5. 6 and 7 we get:

$J_T = 1.2028666625270451\times10^{45}$ Kg.m^2.sec^{-1} 14

$C_0 = 1.1464222821784802\times10^{38}$Kg.m^2 15

$B=\sqrt{[G(M_1 + M_2)]} = 1.9376364278239845\times10^{10}$ (m$^{3/2}$/sec) 16

$E= J_T/(BC_0) = 5.415081346544725\times10^{-4}$ m$^{-3/2}$; 17

$F= (M_2/(1+M_2/M_1))\times(1/C_0) = 1.2264934605867798\times10^{-8}$ m^{-2}; 18

$(\omega/\Omega) = E\times a^{3/2} - F\times a^2 = 499{,}460$

(calculated value at a= $1.9492618530344882\times10^9$ m); 19

Observed value $(\omega/\Omega) = P_{orbit}/P_{spin} = 472{,}759.3047$;

There is a 5.6% discrepancy between the calculated value and the observed value of the ratio of (angular spin velocity of the primary/orbital angular velocity) of the system. At the Clarke's Orbits, Keplers Third Law is exactly satisfied hence even after Kepler Approximation we get exact correspondence at the Clarke's Orbits. The 5.6% discrepancy is within the error of margin of the measured system parameters.

Here the masses are not tightly constrained due to the lack of edge-on view. Instead we have oblique view of the orbital plane which makes the Shapiro delay observation difficult and hence semi-major axis is poorly constrained. Inspite of this poor constraint, the system parameters have satisfied the Architectural Design Rules.

The roots of the spin to orbital equation:
$E\times a^{3/2} - F\times a^2 = 1$ are $a_{G1} = 150.566$m and $a_{G2}=1.94909\times10^9$ m
whereas the present $a_{AB} = 1.9490543729572563\times10^9$ m;
Therefore evolution factor = $(a-a_{G1})/(a_{G2}-a_{G1}) = 0.999979$. 20
Offset w.r.t. the Unity factor is 2.14×10^{-3}%.

This is just as predicted. Gravitational Radiation induced spiral-in tendency opposes the achievement of outer Clarke's configuration perpetually until the two bodies merge finally. The mass ratio is 0.963 hence the secondary almost at a time scale of months/years

evolves asymptotically to the near-outer Clarke's Orbit but it will never settle down into triple synchrony state because of perpetual spiral-in tendency due to Gravitational Radiation. Larger is the mean rate of advancement of the periastron, stronger is the Relativistic nature of the DNSB and hence larger is the spiral-in tendency and hence there is a larger offset from the Unity Evolution Factor and this precisely is obtained by the Architectural Design Rule analysis as shown in Table 6.

Application of Architectural Design Rules to DNSB J0737-3039

All neutron-star binaries are destined to merge because of spiral-in of the components due to the gravitational radiation. Most of the known NS binaries have merger time greater than the age of the Universe hence we cannot witness their merger. But recently discovered J0737-3039 is strongly relativistic double pulsars as is evident from its mean rate of periastron advancement tabulated in Table 6 hence it has merger time of 87My so we will witness its final merger. Here the two spin periods are accurately known [98].
P_b = 8834.53504sec (2.454 hours);
P_{spinA} = 0.022699sec (Age of 'A' component = 210My);
P_{spinB} = 2.7734607 sec (Age of 'B' component = 50My);
Eccentricity (e) = 0.088.

The parameters of the PSR J0737−3039 binary system, and the high timing precision made possible by the narrow pulses of this pulsar, promise to make this system an excellent 'laboratory' for the investigation of relativistic astrophysics, in particular of all the effects that are enhanced by a short orbital period P_b.

Geodetic spin-precession due to curvature of space-time around the pulsar is expected to have a period of 75 yr. This is shorter by ¼ times of the previous minimum spin-precession periods.

The Shapiro Delay should be measurable as the orientation becomes favourable and pulse morphology improves.

Table 11: The Evolution of Pulsar Binary Since its Birth due to Gravitational Radiation

	Orbital period	eccentricity
100My B.P.	3.3h	0.119
Present	2.454h	0.088

This is the largest change observed in orbital elements due to Gravitational Radiation in the sample of known Pulsar Binaries [99]. There are only 6 double NS systems and only 4 will merge in Hubble Time, the other three being PSR 2127+11C, PSR B191+16 and PSR B1534+12 [99].

The mathematical analysis has been done in SOM_Appendix B.

The spin to orbital angular velocity ratio has 0.76542% discrepancy between theory and observation which is acceptable within the margin of error in the measurement of system parameters. The ratio discrepancy is the least in this sample of DNSB because of the fact that the Spin Period of the secondary is accurately known.

The inner and outer Clarke's orbits are:
a_{G1} = 198.36m and a_{G2}=8.789046280437859×10^8 m
whereas a_{AB} =8.788307422131581 ×10^8 m;
Therefore, evolution factor = $(a-a_{G1})/(a_{G2}-a_{G1})$ = 0.9999112261
Offset w.r.t. the Unity Evolution Factor is (8.4×10^{-3})%.

This is just as predicted. In a pulsar binary the mass ratio is greater than 0.2 hence the secondary evolves asymptotically to the near outer Clarke's Orbit on a time scale of months/year but the evolution factor will never be € = 1 because of the spiral-in due to Gravitational Radiation. The spiral-in due to Gravitational Radiation in this strongly relativistic pulsar binary perpetually prevents the system from achieving the final triple synchrony configuration at outer Clarke's Orbit. The strength of relativistic system is expressed by the rate of periastron advancement which in this case is 16.88° per year. Weaker will be the relativistic the system, closer will it be to triple synchrony condition.

Application of Architectural Design Rules to DNSB PSR_B1534+12

Double-Neutron-Star Binary PSR B1534+12 is very similar to Hulse-Taylor Pair except that it is closer to the Earth. Hence it is brighter. Its Pulse Period is shorter and profile narrower. This permits better timing precision. Unlike Hulse-Taylor Pair, here we have edge-on view therefore Shapiro Delay measurement is tightly constrained. Hence, we have 5 PK parameters accurately known. The mathematical analysis is carried out in SOM_Appendix C.

There is 3.75% discrepancy in spin to orbital angular velocity ratio. This is due to low confidence range of System Parameters.

The inner and outer Clarke's Orbits are:
a_{G1} = 140.934m and a_{G2}=2.287421629183039×10^9 m
whereas a_{AB} = 2.2873519882004747×10^9
Therefore, evolution factor = $(a-a_{G1})/(a_{G2}-a_{G1})$ = 0.9999695548096745
Offset w.r.t. the Unity Evolution Factor is (3×10^{-3})%.
This answer is suspect since in mass-mass diagram for PSR B1534+12, the labeled curves in Figure 8 of Reference by illustrates 68% confidence ranges of DD parameters listed in the Table above. Hence it is poorly constrained.
Careful analysis of the timing data for B1534+12 has revealed the presence of unmodeled orbital effects of unknown origin. [77]. This could be the reason for low confidence range for the system parameters.

Application of Architectural Design Rules to DNSB PSR_2127+11C

PSR 2127+11C is found in globular cluster M15 [100]. 50% of 90 known MSP is in Globular Cluster (GC). The high concentrate of stars in the cores of the cluster facilitate the recycling of old neutron stars to MSP. Orbital Period Derivative (Pb') is affected by the acceleration in the cluster potential and hence the system has not proved useful for General Relativity (GR) tests [88].

The mathematical analysis has been done in SOM_Appendix D.

There is 3% discrepancy in calculated and observed values of spin to orbital angular velocity ratio. This is due to poor conditions of measurement in Globular Clusters.
The inner and outer Clarke's Orbits are:
aG1 = 147.588m and aG2=1.97056×10^9 m.
whereas a_{AB} = 1.970478820×10^9 m.
Therefore, evolution factor = $(a-a_{G1})/(a_{G2}-a_{G1})$ = 0.9999588036
Offset from the Unity Factor by (4.12×10^{-3})%.

This has the second largest mean rate of periastron advance hence it has the second largest offset w.r.t. Unity Evolution Factor which is as expected.

Application of Architectural Design Rules to DNSB PSR J1518+4904 and PSR J1811-1736

Both DNSB PSR J1518+4904 and PSR J1811-1736 are mildly

relativistic because of wide separation between the components. The separation of components is one order of magnitude larger than the separation of DNSB studied till now and this distinction arises because of its distinct evolutionary history which we have already discussed in Section 7.3. Because of this wide separation the advance of periastron is only 0.0111°/y and 0.009°/y respectively. This gives rise to undetectable gravitational radiation and merger time much larger than Hubble Time of 13.7Gy. The mathematical analysis of these two wide binaries has been done in SOM_Appendix E and SOM_Appendix F.

The results of inner, outer Clarker's orbits, evolution factor and offset are tabulated in Table 12.

Table 12: Inner (aG1), Outer (aG2) Clarke's Orbits, Evolution Factor (€) and Offset (1-€) of DNSB PSR J1518+4904 and PSR J1811-1736.

PSR	a_{G1}(m)	a_{G2}(m) [$\times 10^{10}$]	€	(1-€)= offset%
J1518+4904	72.2501	1.7001701834454922	0.99999	1×10^{-3}
J1811-1736.	61.9861	2.8767103677018898	0.999997	0.312×10^{-3}

The characteristic ages of these two systems are respectively 16.2Gy and 889My [82]. Since they are mildly relativistic and they are old therefore I have assumed the secondary to be synchronized with the orbital period.

As predicted earlier because of very feeble gravitation radiation induced spiral-in, the binary is comfortably settling down in triple synchrony state with minimum offset.

Discussion

In this paper we have shown that Keplerian Binaries such as compact star binaries NN Serpentis and R W Lacertae have ages respectively >2.38Gy and 11Gy. These large time span has given them enough time for settling in Outer Clarke's Orbit. First it fell into near-outer Clarke's Orbit and then through tidal synchronization and circularization it settled down comfortably in triple synchrony state hence the two compact star binaries have evolved to a perfect score of Unity Evolution Factor. This is not the case with visual binaries such as 61 Cygni (STF 2758AB, WDS 21069+3845) and Alpha Centauri [101,102]. Their separations are 86.4AU and 23.3616AU respectively and eccentricities are 0.4 and 0.579 respectively. Both these star pairs have high eccentricity and unsynchronized components. Because of large separation, tidal interaction is weak and tidal dissipation is feeble hence circularization time and synchronization times are more than Hubble Time. So we can never expect them to fall in triple synchrony state though they have rapidly fallen in near-outer Clarke's Orbit. The calculations have been done for Alpha Centauri in SOM_Appendix I. On a time, scale of months/years it achieved €=0.999854 and offset= (1-€)×100= 14.576×10^{-3} %. This gap has to be bridged in by tidal circularization and tidal synchronization. But the tidal synchronization time scale is more than Hubble Time since it varies as the sixth power of semi-major axis [see SOM_Appendix G]. The circularization time scale is still longer. Hence this gap will never be bridged. This is still satisfying the primary-centric framework except that the binary is too wide to allow synchronization and circularization within Hubble time. Short period binary will invariably have a lower eccentricity because of more powerful tidal interaction.

The distinction between Keplerian and Relativistic Binaries lies in surface gravity of the components. Keplerian Binaries have components with self gravity of 10-6 order whereas NS and BH have surface gravity of the order of 0.2 and 0.5 respectively. In NS binaries, BH binaries or combination of NS+BH give rise to relativistic binaries. In relativistic binaries Strong-field Relativistic Gravitational Theory becomes applicable where by precise measurement of time-of-arrival of the pulses we deduce the five Keplerian Orbital Parameters and the eight Post-Keplerian Parameters. Subsequently 5 Keplerian Parameters and 2 PK parameters will help us constrain the component masses and the geometrical configuration of the DNSB. If we have more than 2 PK parameters, the problem is overdetermined and new GR tests can be carried out such as geodetic precession, mean rate of advance of periastron and orbital decay.

Because of Relativistic effects, DNSB are invariably accompanied with quadrupolar mass Gravitational Radiation. This quadrupolar emission is the dominant mode of energy dissipation as compared to tidal dissipation in Keplerian Binaries. Hence DNSB can asymptotically approach near-outer Clarke's Configuration but can never finally settle in triple-synchrony state resulting in an offset = (1-€). The magnitude of this offset directly depends on the strength of relativistic binaries which in turn can be measured by its relativistic manifestations such as mean rate of advance of periastron(ω') or orbital decay rate (P_b') or by geodetic precession rate. In my paper I have taken mean rate of advance of periastron(ω') as the measure of relativistic strength of the DNSB and tabulated the offset in relation to this quantity in Table 6. As seen in Table 6, the magnitude of offset increases as the mean rate of advance of periastron increases. PSR J0737-3039 exhibits the largest ω' = 16.88°/y and hence it has the largest offset (8.5×10^{-3}%) whereas PSR J1811-1736 the smallest ω' = 0.009°/y and correspondingly it has the least offset (0.312×10^{-3}%).

In all these binaries with mass ratio q > 0.2, sum of the radii of the two components is greater than inner Clatke's Orbit semi-major axis aG1. Hence the formation process is hydro-dynamic instability with much shorter time-scale of formation and inner Clarke's Orbit semi-major axis aG1 has no physical significance [103]. The two components form and fall in near-outer Clarke's Configuration on a time –scale of months/years. How soon they finally settle in triple synchrony state will depend on the strength of tidal interaction and on the mechanism of spin-orbital energy dissipation.

If the mass ratio q < 0.2, then sum of the radii is less than inner Clatke's Orbit semi-major axis aG1 then the formation process is core-accretion with much larger time-scale of formation [103]. Once the two components are formed the secondary is placed at inner Clatke's Orbit semi-major axis aG1 which is an unstable equilibrium orbit because of energy maxima. The secondary can either fall short of aG1 or fall long of aG1 If it falls short of aG1, the secondary gets trapped in a death spiral which is a gravitational runaway contracting spiral. If it falls long of aG1 it gets launched on an expanding spiral trajectory by an impulsive gravitational sling-shot just as it has happened in case of Moon.

Conclusion

In the previous studies we had seen that Planet-Satellite pairs and planetary systems and exo-planetary systems obeyed the Architectural Design Rules based on the new perspective [9,57-61,104]. In the present study we find that Keplerian Binaries as well obey the Architectural Design Rules with the limitation of tidal locking time-scale. The relativistic Binaries always fall in near-outer Clarke's Configuration but they are never allowed to finally settle into the triple synchrony state because of gravitational radiation induced perpetual spiral-in. Hence I can say that this study is a vindication of the Architectural Design Rules proposed by me in 2004_35th COSPAR Scientific Assembly. This Architectural Design Rules will be referred to as Primary-Centric Frame-work [105-116].

Future Direction

The next urgent assignment before me is to test the orbits of the stars in our Milky Way. Do they satisfy the Primary-centric Framework? I predict to find them in inner Clarke's Orbit just as man-made geo-synchronous satellites are in inner geo-synchronous orbit. I will analyze the BH binaries also. They will be in outer Clarke's Configuration but greatly offsite from Unity Evolution Factor due to much more powerful gravitational radiation. I also propose to make Dark Matter correction for massive systems like Galaxies, Clusters and Superclusters, and I will test to see if they fit the computational framework afforded by the primary-centric World View. This may in due course of time be recognized as the common underlying physical process shaping the evolution of this Universe and its sub-systems.

Acknowledgement

I acknowledge the cooperation extended by the Director, IIT, Patna, in letting me use the library facilities of his Central Library. This research has been sponsored by University Grants Commission, Government of India, under Emeritus Fellowship Scheme.

Conflict of Interest

There is no conflict of interest financial or otherwise with anybody.

Supplementary-on-Line Material of: Gravitational Radiation Induced Spiral-in Offsets the Pulsar Pair from its Final Lock-In Position- a New Metric for Relativistic Pulsar Binaries.

The Emergence of Primary-Centric World View and its Grand Vindication by Stellar Binaries- Keplerian Binaries and Relativistic Binaries.

Appendix A. Primary-Centric Analysis of RW Lacertae (GSC 03629-00740)

RW Lac is a detached, eccentric, EA-type, 10.37days orbital period, double-lined eclipsing binary star belonging to the class of Keplerian binaries where mass has been calculated by the Doppler shift in the spectral lines due to the radial velocities of the two components [1]. Here there is no detectable advancement of the periastron hence it has been classified as a Keplerian Binary. The orbits are slightly eccentric indicating that the tidal circularization is not complete during its existence of 11Gy as a binary. The spectral line-widths give observed rotational velocities which indicate triple synchrony state. The components of the binary are old, some-what metal deficient, low mass, main sequence stars with an age of 11Gy.

Table A 1: Globe-Orbit-Spin Parameter of the Two Components of the Keplerian Binary RW Lac

parameters	Primary		Secondary	Ref.
Age		11Gy		
Distance d (pc)		190±10		
Spectral type	G5		G7	1
Stellar mass($\times M_0$)	0.928±0.006		0.87±0.004	1
Stellar Radius (($\times R_0$)	1.186±0.004		0.964±0.004	1
Orbital period(d)		10.3692046±0.0000017 895899.2774 s		1
Semi-major axis(($\times R_0$)		24.32±0.05		1
Rotational Vel (Km/s)	5.8±0.1		4.7±0.1	1
Stellar Spin Period(s)	893580.53		896305.742	1
eccentricity		0.0098±0.0010		1
Angle of inc.(i)		89.45°		1
Tidal locking time	2.92Gy		3.18Gy	1
Apsidal Motion		Undetectable.		
Argument of Periastron		183±11°		

References

1. Lacy Sandberg, Claud H (2005) Absolute Properties of the Eclipsing Binary Star RW Lacertae. The Astronomical Journal 130: 2838-2846.

Here 'a' semi-major axis has been finely tuned to $1.6914857860592089\times10^{10}$m to get the exact fit with the spectroscopically determined orbital parameters. This is within the observed error margin of the nominal value 'a' of 1.691485211×10^{10}m

Substituting the numerical values of the orbit, spin and globe parameters from the Table A.1 into Equation 3, 4, 5 , 6 and 7 of the main text we get:

$J_T = 1.7976528221408725\times10^{45}$ Kg.m^2.sec^{-1} A.1

$C_A = 0.4M_AR^2 = 5.022987799536064\times10^{47}$Kg.m^2 A.2

$B=\sqrt{[G(M_A + M_B)]} = 1.5447231695215513\times10^{10}$ (m$^{3/2}$/sec) A.3

$E= J_T/(BC_A) = 2.3168239656088053\times10^{-13}$ m$^{-3/2}$; A.4

$F= (M_B/(1+M_A/M_A)\times(1/C_A) = 1.7778942574581303\times10^{-18}$ m^{-2}; A.5

$(\omega/\Omega) = E\times a^{3/2} - F\times a^2 = 1$ (calculated value at $a_{AB} = 1.6914857860592089\times10^{10}$m); A.6

Observed value $(\omega/\Omega) = P_{orbit}/P_{spin} = 1$;
The roots of the spin to orbital equation:
$E\times a^{3/2} - F\times a^2=1$ are $a_{G1} = 2.91094\times10^8$ m and $a_{G2}=1.6914857860592075\times10^{10}$ m
whereas $a_{AB} = 1.6914857860592089\times10^{10}$m;
Therefore, evolution factor = $(a-a_{G1})/(a_{G2}-a_{G1}) = € = 1$.

This is just as predicted by Primary-centric World View.

Appendix-B. Primary-centric Analysis of Pulsar Pair J0737-3039

All neutron-star binaries are destined to merge because of spiral-in of the components due to the gravitational radiation. Most of the known NS binaries have merger time greater than the age of the Universe hence we cannot witness their merger. But recently discovered J0737-3039 highly relativistic double pulsars has merger time of 87My so we will witness its final merger.

P_{orbit} = 8834.53504sec (2.454 hours);
P_{spinA} = 0.022699sec (Age of 'A' component = 210My);
P_{spinB} = 2.7734607 sec (Age of 'B' component = 50My);
50My time is less than t_{lock} for a pulsar hence companion pulsar does not synchronize with the orbital period.
Eccentricity (e) = 0.088.

Together with the Relatively Low Radio Luminosity of psr j0737-3039, this Timescale of 87my Implies an Order-Of Magnitude Increase in the Predicted Merger Rate for Double-Neutron-Star Systems In Our Galaxy (and in the Rest of the Universe)

Due to General Theory of Relativity effects there is very large and probably the highest rate of periastron advance. In the Table the rate of advance is tabulated for different binaries.

Table B.1: Apsidal Motion for Different Relativistic Systems [1-3].

Relativistic Binary	Rate of periastron advance	Strength of relativism	Reference
Mercury-Sun	43 arcsec per century	Non-relativistic	3
PSR J0737-3039	16.88° per year	Strongly relativistic	1
PSR 2127+11C	4.4636° per year	Intermediate relativistic	2
PSR 1913+16	4.22° per year	Intermediate relativistic	2
PSR 1534+ 12	1.76° per year	Intermediate relativistic	2
PSR J1518+4904	0.0111° /y	Mildly relativistic	2
PSR1811-1736	0.009°/y	Mildly Relativistic	2

Table B. 2: Globe-Orbit-Spin Parameter of the Two Components of the Pulsar Binary PSR J0737-3039 [4, 5].

parameters	PSR J0737-3039A		PSR J0737-3039B	Ref.
Stellar mass from R(mass ratio) and ω' (×M_0)	1.337		1.25	1
Projected semi-major axis x=aSini/c (s)	1.41504		1.513	1
i (inclination angle)from Calculation		Sin(i) = 0.9990117464274678 87.45253868°		Cal
i (inclination in degree) from Shapiro		87		1
$a_A + a_B = a_{AB}$ (actual separation of A & B) (m)		$8.788307422131581\times10^8$		Cal.
Spin Period of the component(ms)	22.699337855615		2773.4607474	1
Orbital period(d)		0.102251563d 8834.535043s		1
Typical value of Radius (R)	10Km		10Km	2

Here all calculations are carried out considering every system parameter with 16 significant digits in order to get the correspondence between theory and observation.

The shape of the Shapiro Delay is given as follows [1].

$$shape = s = Sin(i) = T_0^{-\frac{1}{3}} \times \left(\frac{a_P \sin i}{\frac{M_C}{M_0}} \right) \left(\frac{P_b}{2\pi} \right)^{-\frac{2}{3}} ((M_P + M_C)/M_0)^{\frac{2}{3}} \quad B.1$$

$$\text{Here } T_0 = \frac{GM_0}{c^3} = 4.925490947 \times 10^{-6} sec$$

Here G = Gravitational Constant and c= velocity of light in vacuum
and M_0 =1.988797242×10^{30}Kg.
Substituting the parameter values in Eq.B.1 we get Sin(i) as:
Sin (i) = 0.9990117464274678 and i = 87.45253868°
Keplerian Orbital Parameters give us the mass function [Damour & Deruelle (1986)]:

$$M_f = \frac{M_B Sin(i)}{(M_A + M_B)^2} = \frac{4\pi^2 (aSin\, i)^3}{GP_{Orbit}^2} \qquad B.2$$

Let Periastron advance be solely due to General Relativity that is ω' = ω'GR . Using the following relation, total mass is calculated:

$$M_A + M_B = \frac{(P_{Orbit})^{5/2}}{2\pi G} \left[\frac{(1-e)^2 c^2 \omega'}{6\pi} \right]^{3/2} = 2.58 M_0 \qquad B.3$$

Masses have been constrained to : M = $2.587M_0$, M_A = $1.337M_0$ and M_A = $1.25M_0$

Total angular momentum:

$$J_T = 0.4 M_A M_{\square} R_{\square}^2 \times \left(\frac{2\pi}{P_{\square spinA}} \right) + 0.4 M_B R^2 \times \left(\frac{2\pi}{P_{spinB}} \right) + \frac{M_B}{1 + \frac{M_B}{M_A}} a_{AB}^2$$

$$\times \left(\frac{2\pi}{P_{orbit}} \right) \qquad B.4$$

Substituting the numerical values of the orbit, spin and globe parameters from the Table into Equation 3, 4, 5, 6 and 7 of the main text we get:

$J_T = 7.057654719135262 \times 10^{44}$ Kg.m^2.sec^{-1}

$C_A = 0.4 M_A R^2 = 1.0636087650216 \times 10^{38}$Kg.m^2 B.5

$B = \sqrt{[G(M_A + M_B)]} = 1.852908746196243 \times 10^{10}$ (m$^{3/2}$/sec) B.6

$E = J_T/(BCA) = 3.581166132606733 \times 10^{-4}$ m$^{-3/2}$; B.7

$F = (M_B/(1+M_B/M_A) \times (1/C_A) = 1.2079628913799769 \times 10^{-8}$ m^{-2}; B.8

$(\omega/\Omega) = E \times a^{3/2} - F \times a^2 = 392177$ (calculated value at $a_{AB} = 8.788307422131581 \times 10^8$ m); B.9

Observed value $(\omega/\Omega) = P_{orbit}/P_{spin} = 389,197.9184$;

The 0.76542% discrepancy between theory and observation is acceptable within the margin of error in the measurement of system parameters.

The roots of the spin to orbital equation:

$E \times a^{3/2} - F \times a^2 = 1$ are $a_{G1} = 198.36$m and $a_{G2} = 8.789046280437859 \times 10^8$ m

whereas $a_{AB} = 8.788307422131581 \times 10^8$ m;

Therefore, evolution factor = $(a-a_{G1})/(a_{G2}-a_{G1}) = 0.9999112261$

Off the Unity Factor by (8.4×10^{-3})%.

This is just as predicted. In a pulsar binary the mass ratio is nearly UNITY hence the secondary evolves asymptotically to the outer Clarke's Orbit on a time scale of months/year. It will never be UNITY because the spiral-in due to Gravitatinal Radiation. The spiral-in due to Gravitational Radiation in this strongly relativistic pulsar binary continuously prevents the system from achieving the final triple synchrony configuration at outer Clarke's Orbit. The strength of relativism of the system is expressed by the rate of periastron advancement which in this case is 16.88° per year. Weaker will be the relativism of the system, closer will it be to triple synchrony condition.

Measurement of projected separation x_A and x_B gives us the mass ratio $R = M_A/M_B = x_B/x_A$. This relation is valid in any theory of gravity. This provides a stringent and new constraint for tests of gravitational theories. The Evolution of Pulsar Binary since its birth due to Gravitational Radiation is given in Table 11 in the main Text. This is the largest change observed in orbital elements due to Gravitational Radiation in the sample of known Pulsar Binaries [1]. There are only 5 double NS systems and only 3 will merge within Hubble Time [1,6].

References

1. Burgay M, Amico ND, Possenti A, Manchester RN, Lyne AG, et al. (2003) An increased estimate of the merger rate of double neutron stars from observations of a highly relativistic system. Nature 426: 531-533.
2. Lyne AG, Burgey M, Kramer M (2004) A Rare Laboratory for Relativistic Gravity and Plasma Physics. Science 303: 1153-1157.
3. Stairs Ingrid H (2003) Testing General Relativity with Pulsar Timing. Living Reviews in Relativity, Published by Max Planck Institute for Gravitational Physics 6: 5.
4. Taylor JH (1992) Pulsar Timing and Relativistic Gravity. Philosophical Transactions of Royal Society of London:Physical Sciences and Engineering 341: 117-134.
5. Tiec AL, Mroue AH, Barack L (2011) Periastron Advance in Black Hole Binaries. ar Xiv 1106: 3278v2
6. Damour T, Deruelle N (1986) General relativistic celestial mechanics of binary systems. II The post-Newtonian timing formula. Ann Inst H Poincar´e (Phisique Th´eorique) 44: 263-292.

Appendix_C. Primary-centric Analysis of Pulsar Pair PSR1534+12

Double-Neutron-Star binary PSR B1534+12 is very similar to Hulse-Taylor Pair except that it is closer to the Earth. Hence it is brighter. Its Pulse Period is shorter and profile narrower. This permits better timing precision. Unlike Hulse-Taylor Pair, here we have edge-on view therefore Shapiro Delay measurement is tightly constrained. Hence, we have 5 PK parameters accurately known.

Table C.1: Orbital Parameters for PSR B1534+12 in the DD Framework

Parameters	Value	
Orbital Period_P_b (d)	0.420737299122(10)	36351.70264s
Projected semi-major axis_x_p(l-s)	3.729464(2)	
Eccentricity_e	0.2736775(3)	
Longitude of periastron_ω(deg)	274.57679(5)	
Epoch of periastron_T_0(MJD)	50260.92493075(4)	
Advance of periastron_ω'(deg.y^{-1})	1.755789(9)	
Gravitational red shift_γ(ms)	2.070(2)	
Orbital period derivative$(P_b')_{obs}$($\times10^{-12}$s/s)	-0.137(2)	
Shape of Shapiro delay_s	0.975(7)	
Range of Shapiro delay_r (μs)	6.7(1.0)	

Here all calculations are carried out considering every system parameter with 16 significant digits in order to get the correspondence between theory and observation [1].

Substituting the parameter values in Eq.B.1 we get Sin(i) as:
Sin(i) = 0.9776066344914563
Inclination angle = (i) = 77.852°

Table C.2: Globe-Orbit-Spin Parameter of the Two Components of the Pulsar Binary PSR B1534+12 [1].

parameters	PSR B1534+12A		PSR B1534+12B	Ref.
Stellar mass (×M0)	1.34(7)		1.34(7)	1
Projected semi-major axis x=apSini/c (s)	3.7294642		3.729462	1
Sin(i) (inclination in degree) from the formula		0.9776066344914563 (i) = 77.852°		Cal
$a_A + a_B = a_{AB}$ (actual separation of A & B) (m)		$2.2873519882004747\times10^9$		Cal.
Spin Period of the component(ms)	37.9		1000 (assumed)	1
Orbital period(d)		0.420737299122(10)		1
Typical value of Radius (R)	10Km		10Km	2

Substituting the numerical values of the orbit, spin and globe parameters from Table C.2. in Equation 3 of the main text, we get:

$J_T = 1.2113114806007812\times10^{45}$ Kg.m^2.sec^{-1} C.1

$C_A = 0.4M_AR^2 = 1.0715639539896\times10^{38}$Kg.$m^2$ C.2

$B=\sqrt{[G(M_A + M_B)]} = 1.8908392666978065\times10^{10}$ ($m^{3/2}$/sec) C.3

$E= J_T/(BC_A) = 5.978374608292618\times10^{-4}$ $m^{-3/2}$; C.4

$F= (M_B/(1+M_B/M_A)\times(1/C_A) = 1.2499999999999998\times10^{-8}$ m^{-2}; C.5

$(\omega/\Omega) = E\times a^{3/2} - F\times a^2 = 995577$ (calculated value at $a_{AB} = 2.2873519882004747\times10^9$); C.6

Observed value $(\omega/\Omega) = P_{orbit}/P_{spin} = 959148$

The 3.75% discrepancy is due to uncertainty in System Parameters.
The roots of the spin to orbital equation:
$E\times a^{3/2} - F\times a^2 = 1$ are $a_{G1} = 140.934$m and $a_{G2} = 2.287421629183039\times10^9$ m
whereas $a_{AB} = 2.2873519882004747\times10^9$
Therefore, evolution factor = $(a-a_{G1})/(a_{G2}-a_{G1}) = 0.9999695548096745$
Off the Unity Factor by (3×10^{-3})%.
This answer is suspect since in mass-mass diagram for PSR B1534+12, the labeled curves in Figure 8 of Reference illustrates 68% confidence ranges of DD parameters listed in the Table above [1, 2].

References
1. Stairs IH, Thorsett SE, Taylor JH, Wolszczan A (2002) Studies of the Relativistic Binary Pulsar PSR B1534+12: I. Timing Analysis. Astrophys J 581: 501-508.
2. Wolszczan A (1991) A nearby 37.9 ms radio pulsar in a relativistic binary system. Nature 350: 688-690.

Appendix_D. Primary-centric Analysis of Pulsar Pair PSR2127+11C

Table D 1: Orbital Parameters for PSR 2127+11C in the DD Framework Taken from [1].

Parameters	Value	
Orbital Period_P_b (d)	0.335282057(2)	28968.36974(2)s
Projected semi-major axis_x_p(l-s)	2.51857(21)	
Eccentricity_e	0.681388(5)	
Longitude of periastron_ω(deg)	316.3629	
Epoch of periastron_T_0(JD)	2447633.02	
Advance of periastron(Apsidal Motion)_ω'(deg.y^{-1})	4.4636	
Gravitational red shift(Einstein Delay)_γ(ms)	0.00467	
Orbital period derivative(P_b')$_{obs}$($\times10^{-12}$s/s)	-3.937	

Table D 2: Globe-Orbit-Spin Parameter of the Two Components of the Pulsar Binary PSR 2127+11C [1,2]

parameters	PSR 2127+11C_A		PSR 2127+11C_B	Ref.
Stellar mass ($\times M_0$)	1.348(76)	M1+M2=2.7121(6)	1.363(40)	1
Projected semi-major axis x=apSini/c (l-s)	2.51857(21)		2.4915280(22)	1
Sin(i) (inclination in degree) from the formula		0.7622463204315938 (i)=49.66263074°		Cal
$a_A + a_A = a_{AB}$ (actual separation of A & B) (m)		$1.9704788205973256\times10^9$		Cal.
Spin Period of the component(ms)	30.5292951283(3)		1000 (assumed)	1
Orbital period(s)		28968.36974(2)		1
Typical value of Radius (R)	10Km		10Km	2

Using Eq. B1 Formula we get Sin(i)= 0.7622463204315938
Substituting the numerical values of the orbit, spin and globe parameters from Table D.2 in Equation 1, 2, 3, 4, 5 and 6 of the main text , we get:

$J_T = 1.135641438\times10^{45}$ Kg.m^2.sec^{-1} D.1

$C_A = 0.4M_AR^2 = 1.072964067\times10^{38}$Kg.$m^2$ D.2

$B=\sqrt{[G(M_A + M_B)]} = 1.897201547\times10^{10}$ ($m^{3/2}$/sec) D.3

$E= J_T/(BCA) = 5.578823003\times10^{-4}$ $m^{-3/2}$; D.4

$F= (M_B/(1+M_A/M_A)\times(1/C_A) = 1.25674739\times10^{-8}$ m^{-2}; D.5

$(\omega/\Omega) = E\times a^{3/2} - F\times a^2 = 978140$ (calculated value at $a_{AB} = 1.970478820\times10^9$); D.6

Observed value $(\omega/\Omega) = P_{orbit}/P_{spin} = 948871.2274$

The 3% discrepancy is due to poor conditions of measurement in Globular Clusters.
The roots of the spin to orbital equation:
$E\times a^{3/2} - F\times a^2=1$ are a_{G1} = 147.588m and $a_{G2}=1.97056\times109$ m.
whereas $a_{AB} = 1.970478820\times10^9$ m.
Therefore, evolution factor = $(a-a_{G1})/(a_{G2}-a_{G1}) = 0.9999588036$
Offset from the Unity Factor by (4.12×10^{-3})%.

References
1. Stairs, Ingrid H (2003) Testing General Relativity with Pulsar Timing. Living Reviews in Relativity Published by Max Planck Institute for Gravitational Physics 6: 5.

2. Paradijs J, Van del Heuvel EPJ, Kuulkers E, Proceedings of the 165th Symposium of the International Astronomical Union: Compact Stars in Binaries 279-285.

Appendix E_PSR J1518+4904

Table E 1: Orbital Parameters for PSR J1518+4904 in the DD Framework [1].

Parameters	Value	Ref
Epoch Period(MJD)	49894.00	1
Spin Period of the Pulsar(ms)	40.93498826871(6)	1
Spin Period Derivative (s/s)	$<4\times10^{-20}$	1
Orbital Period_P_b (d)	8.63400485(5)	1
Projected semi-major axis_x_p(l-s)	20.044003(4)	1
Eccentricity_e	0.2494849(3)	1
Longitude of periastron_ω(deg)	342.46217(8)	1
Epoch of periastron_T0(MJD)	49896.246989(2)	1
Advance of periastron(Apsidal Motion)_ω'(deg.y-1)	0.0111(2)	1
Total Mass M= M_A+M_B	2.62(7)M_0	1
Merger Time(yr)	2.4×10^{12}	1

References

1. Nice DJ, Sayer RW, Taylor JH (1996) PSR J1518+4904: A Mildly Relativistic Binary Pulsar System. Ap J 466: L87.

Table E 2: Globe-Orbit-Spin Parameter of the Two Components of the Pulsar Binary PSR J1518+4904

parameters	PSR J1518+4904_A		PSR J1518+4904_B	Ref.
Stellar mass (×M_0)	1.314665610344959		1.3123343896550408	calculated
Projected semi-major axis x=apSini/c (l-s)	20.044003(4)		20.07960942	calculated
Sin(i) (inclination 'i' in degree) from the formula		0.7075102256 (45°)		calculated
a_A+ a_A = a_{AB} (actual separation of A & B) (m)		$1.7001530178926395\times10^{10}$		calculated
Spin Period of the component	40.934988268716 ms		8.634004855d = 745978.0195s†	1
Orbital period		8.634004855d = 745978.0195		1
Typical value of Radius (R)	10km		10km	Assumed (Stairs 2003)

†Companion has been assumed to be in captured rotation since the characteristic age of the Pulsar Pair is 16.2Gy which is long enough to allow the companion to despin to synchrony with the orbital period [1].

Here the calculations have to be done on the basis of 16 significant decimal digits
Substituting the numerical values of the orbit, spin and globe parameters from the Table E.2, in Equation 3, 4, 5 , 6 and 7 we get:

$J_T = 3.179964704121239\times10^{45}$ Kg.m2.sec^{-1} E.1

$C_A = 0.4M_AR^2 = 1.045841472\times10^{38}$Kg.m^2 E.2

$B=\sqrt{[G(M_A + M_B)]} = 1.8671785661028774\times10^{10}$ (m$^{3/2}$/sec) E.3

$E= J_T/(BC_A)= 1.6284355950638167\times10^{-3}$ m$^{-3/2}$; E.4

$F= (M_B/(1+M_B/M_A)\times(1/C_A) = 1.2488905776586211\times10^{-8}$ m^{-2}; E. 5

$(\omega/\Omega) = E\times a^{3/2} - F\times a^2 = 18.2238\times10^6$ (calculated value at $a_{AB} = 1.700153017892639\times10^{10}$m); E.6

Observed value $(\omega/\Omega) = Porbit/Pspin = 18.2235\times10^6$
There is 1.646×10^{-3} % discrepancy is insignificant discrepancy in the observed and calculated values.
The roots of the spin to orbital equation:
$E\times a^{3/2} - F\times a^2=1$ are a_{G1} = 72.2501m and $a_{G2}=1.7001701834454922\times10^{10}$ m.

whereas $a_{AB} = 1.7001530178926395\times10^{10}$ m.
Therefore evolution factor = $(a-a_{G1})/(a_{G2}-a_{G1}) = 0.99999$
Offset from the Unity Factor by (1×10^{-3})%.

Appendix F_PSR J1811-1736

Table F 1: Orbital Parameters for PSR J1811-1736 in the DD Framework [1].

Parameters	Value	Ref.
Epoch Period (MJD)	51050.0	1
Spin Period of the Pulsar(s)	0.104181954734(3)	1
Spin Period Derivative (s/s)	$1.8(6)\times10^{-18}$	1
Orbital Period_P_b (d)	18.779168(4)	1
Projected semi-major axis_x_p(l-s)	34.7830(4)	1
Eccentricity_e	0.82802(2)	1
Longitude of periastron_ω(deg)	127.661(2)	
Epoch of periastron_T_0(MJD)	51044.03702(3)	1
Advance of periastron(Apsidal Motion)_ω'(deg.y^{-1})	0.009(2)	1
Orbital decay(s/s)	<3×10-11	1
d(kpc)	6(1)	1
Total mass M (×M_0) = MA + MB	2.6(9)	1
Mass Function m(f)	0.128	1
Merger Time(y)	1012	1

References

1. Lyne AG, Camilo F, Manchaster RN (2000) The Parkes Mutibeam Pulsar Survey:PSR J1811-1736 a pulsar in a highly eccentric system, Monthly Notices of Royal Astronomical Society. 312: 698-702.

Table F 2: Globe-Orbit-Spin Parameter of the Two Components of the Pulsar Binary PSR J1811-1736

parameters	PSR J1811-1736_A		PSR J1811-1736_B	Ref.
Stellar mass (×M_0)	1.39		1.3	cal
Projected semi-major axis x=apSini/c (l-s)	34.7830(4)		37.19109662	cal
Sin(i) from the formula		0.7500707692 (i) = 48.5965°		cal
$a_A + a_B = a_{AB}$ (actual separation of A & B) (m)		$2.87670140523988\times10^{10}$		cal
Spin Period of the component(s)	0.104181954734(3)s		18. 779168d= 1622520.115s†	1
Orbital period(s)		18.779168d 1622520.115s		1
Typical value of Radius (R)	10km		10km	Stairs 2003

† Companion has been assumed to be in captured rotation since the characteristic age of the Pulsar Pair is 887My enough to allow the companion to despin to synchrony with the orbital period.

Here the calculations have to be done on the basis of 16 significant decimal digits
Substituting the numerical values of the orbit, spin and globe parameters from Table F.2 in Equation 3, 4, 5, 6 and 7 we get:

$J_T = 4.2813073634934414\times10^{45}$ Kg.m^2.sec^{-1} F.1

$C_A = 0.4M_AR^2 = 1.1057712665519998\times10^{38}$ Kg.m^2 F.2

$B=\sqrt{[G(M_A + M_B)]} = 1.8894350041448776\times10^{10}$ ($m^{3/2}$/sec) F.3

$E= J_T/(BC_A) = 2.049175478554133\times10^{-3}$ $m^{-3/2}$; F.4

$F= (M_B/(1+M_B/M_A)\times(1/C_A) = 1.2081784386617102\times10^{-8}$ m^{-2}; F. 5

$(\omega/\Omega) = E\times a^{3/2} - F\times a^2 = 1.557481469140625\times10^7$
(calculated value at a_{AB} =2.87670140523988 $\times10^{10}$m); F.6
Observed value $(\omega/\Omega) = P_{orbit}/P_{spin} = 1.557390739\times10^7$

There is 5.8×10^{-3} % discrepancy is insignificant discrepancy in the observed and calculated values.
The roots of the spin to orbital equation:
$E\times a^{3/2} - F\times a^2=1$ are a_{G1} = 61.9861m and a_{G2}=2.8767103677018898$\times10^{10}$ m.
whereas a_{AB} = 2.87670140523988 $\times10^{10}$ m.
Therefore, evolution factor = $(a-a_{G1})/(a_{G2}-a_{G1})$ = 0.999997
Offset from the Unity Factor by (0.312×10^{-3})%.

Appendix G_Tidal Locking Time of the Companions of DNSB.
G.1. Tidal Locking Time Scale of Planets and Planet Hosting Star.
Table G 1: Globe & Orbit Parameters of the Eight Planets and Pluto.

Planets	a($\times10^9$m)	α (inclination angle in degress)	Φ (obliquity angle in degrees)	P_1(d)	P_3(d)	m (kg)	ρ + (Kg/m^3)
Mercury	57.9	7.00	7.00	88	58.6	3.3 x 10^{23}	5430
Venus	108.2	3.39	177.4	224.6	-243	4.87 x 10^{24}	5250
Earth	149.6	0.01	23.5	365.25	0.9973	5.97 x 10^{24}	5520
Mars	227.9	1.85	24	686.69	1.026	6.42 x 10^{23}	3930
Jupiter	778.3	1.31	3.1	4,331.865	0.41	1.90 x 10^{27}	1330
Saturn	1,427	2.49	26.7	10,760.265	0.43	5.69 x 10^{26}	710
Uranus	2,870	0.77	97.9	30,684.6525	-0.69	8.86 x 10^{25}	1240
Neptune	4,479	1.77	29.6	60,193.2	0.72	1.02 x 10^{26}	1670
Pluto	5,914	17.15	118	90,801.5	-6.387	1.46 x 10^{22}	2290

References
1. Peter Goldreich, Steven Soter (1966) Q in the Solar System. ICARUS 5: 1-375-389.
2. Gladman Brett, Quinn D Dane, Nicolson Phillip, Rand Richard (1996) Synchronous Locking of tidally Evolving Satellites. ICARUS 122: 166-192.

Table G 2: Seismic Parameters of the Eight Planets and Pluto [1,2]

	a($\times10^9$m)	m (kg)	ρ + (Kg/m^3)	Q	R+ ($\times10^6$m)	g(m/s^2)	ω(ini) assumed
Mercury	57.9	3.3 x 10^{23}	5430	100	2.439	3.7	3.64×10^{-6}
Venus	108.2	4.87 x 10^{24}	5250	100	6.051	8.87	3.64×10^{-6}
Earth	149.6	5.97 x 10^{24}	5520	100	6.378	9.79	3.5×10^{-4}
Mars	227.9	6.42 x 10^{23}	3930	100	3.397	3.71	3.5×10^{-4}
Jupiter	778.3	1.90 x 10^{27}	1330	6×10^4	71.492	24.8	3.5×10^{-4}
Saturn	1,427	5.69 x 10^{26}	710	6×10^4	60.268	10.45	3.5×10^{-4}
Uranus	2,870	8.68 x 10^{25}	1240	6×10^4	25.559	8.86	3.5×10^{-4}
Neptune	4,479	1.02 x 10^{26}	1670	6×10^4	24.764	11.09	3.5×10^{-4}
Pluto	5,914	1.46 x 10^{22}	2290	6×10^4	1.123	0.77	3.5×10^{-4}

Table G 3: The Seismic Parameters in Tidal Second Order Love Number (k2)

	μ*(N/m^2)	<ρ>(Kg/m^3)	g(m/s^2)	R2(($\times10^6$m))	k_2
Mercury	3×10^{10}	5430	3.7	2.439	0.22
Venus	3×10^{10}	5250	8.87	6.051	0.746
Earth	3×10^{10}	5520	9.79	6.378	0.82
Mars	3×10^{10}	3930	3.71	3.397	0.22
Jupiter	4×10^9	1330	24.8	71.492	1.476
Saturn	4×10^9	710	10.45	60.268	1.38
Uranus	4×10^9	1240	8.86	25.559	1.321.
Neptune	4×10^9	1670	11.09	24.764	1.385

Pluto	3×10^{10}	2290	0.77	1.123	0.01

Table G 4: The parameters in Tidal Lock Time-Scale (Mass of our Sun=1.988797242×10^{30}Kg)

	<ρ>(Kg/m^3)	ω(ini) assumed	a(×10^9m)	Q	k_2	T_{lock} (y)
Mercury	5430	3.64×10^{-6}	57.9	100	0.22	14.44M
Venus	5250	3.64×10^{-6}	108.2	100	0.746	175.5M
Earth	5520	3.5×10^{-4}	149.6	100	0.82	112G
Mars	3930	3.5×10^{-4}	227.9	100	0.22	3739G
Jupiter	1330	3.5×10^{-4}	778.3	6×10^4	1.476	179T
Saturn	710	3.5×10^{-4}	1,427	6×10^4	1.38	3.89P
Uranus	1240	3.5×10^{-4}	2,870	6×10^4	1.321.	470P
Neptune	1670	3.5×10^{-4}	4,479	6×10^4	1.385	9×10^{21}
Pluto	2290	3.5×10^{-4}	5,914	6×10^4	0.01	9×10^{24}

According to Primary-centric view all planets are born in a synchronous orbits that is the spin period = orbital period of the planet around the Sun. But subsequently due to giant impact from left-over planetesimals, the planets have been spun up and in case of Venus, Uranus and Pluto they have acquired retrograde motion. After the spin-up, due to tidal heating the planets are being spun down and the time taken for locking in with the orbital period is 'locking time' T_{lock} .

$$t_{lock} = \frac{16\rho\omega a^6 Q}{45Gm_p^2 k_2} \qquad G.1$$

Where ρ = density of the secondary; ω= initial spin rate of the secondary; a= semi-major axis of the orbit; Q = dissipation factor of the secondary body; G = Gravitational Constant; m_P = mass of the primary; k_2 = tidal second order Love Number of the secondary;
For terrestrial planets and satellites : Q = 10 to 500;
For Jovian Planets: $Q = 6\times10^4$;
Tidal Second Order Love Number :

$$k_2 = \frac{3/2}{1 + [\frac{19\mu^*}{2 < \rho > gR_2}]} \qquad G.2$$

Surface gravity = $g = (GM_2)/(R_2^2)$; <ρ> = mean density; μ* = rigidity;
For rocky objects rigidity $\mu^* = 3\times10^{11}$ dyne/cm^2 = 3×10^{10}N/m^2;
For Icy Objects $\mu^* = 4\times10^{10}$ dyne/cm^2 = 4×10^9N/m^2;
R_2 = radius of the secondary.

Using Eq.G.1 and Eq.G.2 and using the parameters given in Table G.4 the locking time-scale is determined. As seen in Table G.4, proximity of our Sun helps the planet lock-in the orbital period in a reasonable time. For Earth and beyond the lock-in time scale is greater than Hubble Time hence by tidal interaction due to our Sun the planets Earth and beyond will never lock-in. In case of Earth the tidal drag due to our Moon has spun-down our Earth from 5 hours to 24 hours spin-period. So lock-in time due to tidal drag is a very strong function of the proximity of the two bodies.

G.3. Lock-in Time Scale of White Dwarf Pairs.
The same formula G.1 and G.2 provided we get the proper values of Q and k2 can be constrained.

G.3. Lock-in Time Scale for Pulsar Pairs.
[Bildstem, Lars and Curt Cutlar (1992)] It states that for NS mass > 1.2M0 , tidal synchronization time exceeds the gravitational decay time so that Neutron Star cannot be tidally locked prior to tidal disruption of NS regardless of internal viscosity.

For smaller mass NS i.e. for mass less than 1.2M0 , a very large Kinematic Viscosity is required for tidal locking. In Black Hole(BH)+Neutron Star(NS) or in NS+NS, during mass transfer phase when NS reaches tidal radius mass transfer will be unstable and the instability will destroy the NS in a few orbital periods. For NS mass < 0.5M0 , mass transfer at tidal radius is stable.

Som_Appendix H. Theoretical Formulation of the Natural Period of a Tidally Oscillating Earth.
Any tidal perturbation by the most dominant body nearest to the Earth will cause tidal bulges as shown Figure H.1.

The mass of the Earth is (assuming a symmetrical biaxial ellipsoid) [Deakins & Hunter (2010)]:

$$M_+ = \frac{4\pi}{3} a^2 b\rho \qquad H.1$$

Where a= semi-major axis of the Earth, b = semi-minor axis of the Earth;
We assume a homogeneous density of the Earth = ρ.

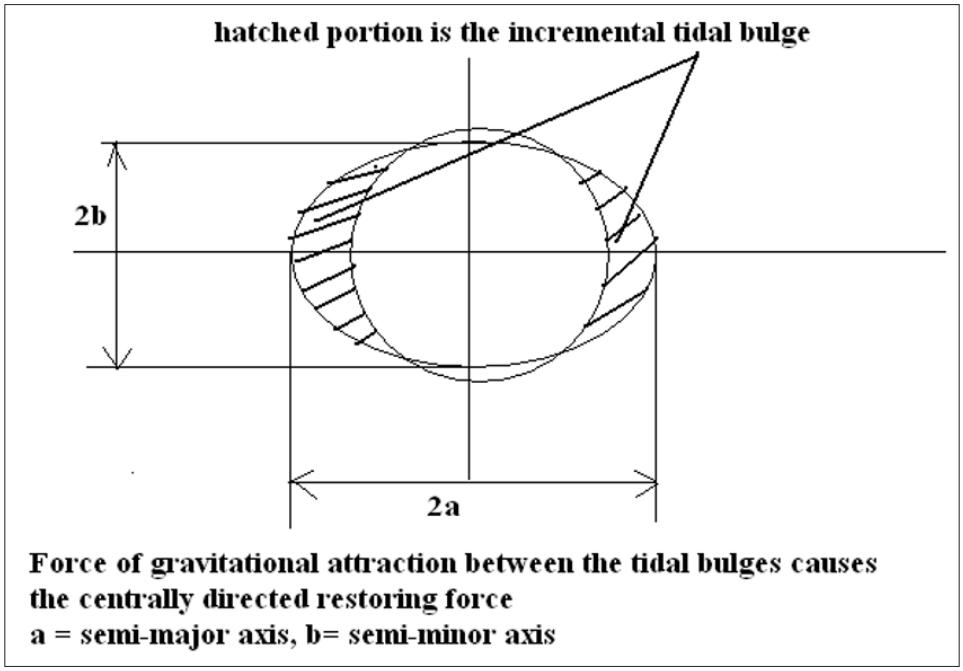

Figure H 1: The tidal perturbation of the Earth by the Nearest Dominant Body. [BP2(2).eps]

The total mass of the two symmetrical bulges = $2M_{Bulge} = \frac{4\pi}{3} a^2 b\rho e^2 \qquad H.2$

Here e = eccentricity and $e^2 = \frac{a^2 - b^2}{a^2} \qquad H.3$

Substituting Eq.H1 in Eq.H2 :
$2M_{Bulge} = e^2 M_+$ H.4

The distance between the center of masses of the two symmetrical tidal bulges = (a+b);

Therefore, the centrally directed restoring force = $F_{restoring} = -\frac{GM_{Bulge}M_{Bulge}}{(a+b)^2} \qquad H.5$

Substituting Eq.H.3 and Eq. H.4 in Eq.H.5 we get the following:

$$F_{restoring} = -\frac{GM_+^2}{4a^4} \times a^2 (1 - \frac{b}{a})^2 \qquad H.6$$

Opening the whole square and neglecting the term of second order of smallness we get:

$$F_{restoring} = -\frac{GM_+^2}{4a^2} \times \left[1 - \frac{2b}{a}\right] \qquad H.7$$

Let (a-b) = Δx = magnitude of incremental perturbation.
Writing the equation of motion the tidally oscillating Earth we get:

$$M_+ \frac{d^2\Delta x}{dt^2} = -\frac{GM_+^2}{4a^2} \times \left[1 - \frac{2b}{a}\right]$$

$$\text{Or } M_+ \frac{d^2\Delta x}{dt^2} = -\frac{GM_+^2}{4a^2} \times \left[\frac{\Delta x - b}{a}\right]$$

$$\text{Or } \frac{d^2\Delta x}{dt^2} = -\frac{GM_+}{4a^3} \times \Delta x + \frac{GM_+}{4a^3} \times b \qquad H.8$$

Eq. H.8 is an ordinary second order linear differential equation . It has a transient response and a steady state response. The transient response is a sine wave with an angular frequency given by Eq. H.9:

$$\sqrt{\frac{GM_+}{4a^3}} = \frac{2\pi}{P_{nat}} = 6.197683211 \times 10^{-4}\ \frac{1}{sec} \qquad H.9$$

Therefore, natural period of oscillation of tidally perturbed Earth = 2.8 hours.
If we take stratified Earth the period of tidally perturbed Earth = 2.5 hours

SOM_Appendix I. Primary Centric Analysis of Alpha Centauri – Keplerian star binary

Table I 1: Globe-Spin-Orbit Parameters

Parameters	Star_A		Star_B
Mass ($\times M_0$)	1.1		0.907
Radius($\times R_0$)	1.227		0.885
Luminosity($\times L_0$)	1.519		0.5
Metallicity(%of Sun)	151		160
Age (Gy)	4.85		4.85
P_{spin}(d)	22		41
P_b(y)		79.71	
a (arcsec)		17.57" ±0.022	
a(AU)		23.3616	
Eccentricity e		0.5179	

Substituting the system parameters from Table I.1 into Eq. 3,4, 5,6 and 7 in the Main Text we get:

$J_T = 3.01663\times10^{46}$ Kg.m^2.sec^{-1} I.1

$C_A = 0.4M_AR^2 = 6.37275 \times10^{47}$ Kg.m^2 I.2

$B=\sqrt{[G(M_A + M_B)]} =1.632035131\times10^{10}$ (m$^{3/2}$/sec) I.3

$E= J_T/(BC_A)= 2.90045\times10^{-12}$ m$^{-3/2}$; I.4

$F= (M_B/(1+M_T/M_A)\times(1/C_A) =1.55137\times10^{-18}$ m^{-2}; I.5

$(\omega/\Omega) = E\times a^{3/2} - F\times a^2 = 1382.14$
(calculated value at $a_{AB} =3.4949\times10^{12}$ m); I.6
Observed value $(\omega/\Omega) = P_{orbit}/P_{spin} = 1323.34$

There is 4.44×10^{-3} % discrepancy is insignificant discrepancy in the observed and calculated values.
The roots of the spin to orbital equation:
$E\times a^{3/2} - F\times a^2=1$ are $a_{G1} = 4.92923\times10^7$ m and $a_{G2}=3.4954\times10^{12}$ m.
whereas $a_{AB} = 3.4949\times10^{12}$ m.
Therefore, evolution factor = $(a-a_{G1})/(a_{G2}-a_{G1}) = 0.999854$
Offset from the Unity Factor by $(14.5761\times10^{-3}$)%.

References

1. Stephenson FR, Houldon M A (1986) Atlas of Historical Eclipse Maps Cambridge University Press. https://www.cambridge.org/in/universitypress/subjects/physics/history-philosophy-and-foundations-physics/atlas-historical-eclipse-maps-east-asia-1500-bcad-1900?format=HB&isbn=9780521267236.
2. Stephenosn FR (2003) Historical Eclipses and Earth's Rotation. Astronomy & Geophysics 44: 2.22-2.27.
3. Morrison LV (1978) Tidal Deceleration of the Earth's Rotation Deduced from Astronomical observations in the Period AD 1600 to the Present. Tidal Friction 22-27.
4. Jong T De, Soldt WH Van (1989) The Earliest known Solar Eclipse record redated. Nature 338: 238-240.
5. Darwin GH (1879) On the precession of a viscous spheroid and on the remote history of the Earth. Philosophical Transactions of Royal Society of London 170: 447-530.
6. Darwin GH (1880) On the secular change in the elements of the orbit of a satellite revolving about a tidally distorted planet. Philosophical Transactions of Royal Society of London 171: 713-891.
7. Zoghbi, Jean Paul A (2011) Quantization of Planetary Systems

and its dependence on Stellar Rotation. Publication of Astronomical Society of Australia 28: 177-201.
8. Radlick R, Thompson D, Lockwood G (1987) The activity, variability and rotation of lower main-sequence Hydaes Stars. AJ 321: 459.
9. Sharma BK, Ishwar B (2004B) A New Perspective on the Birth and Evolution of our Solar System based on Planetary Satellite Dynamics. 35th COSPAR Scientific Assembly.
10. Ida S, Canup RM, Stewart, G R (1997) Lunar Accretion from an impact-generated disk. Nature 389: 353-357.
11. Hartmann (1978) The Cosmic Journey. Wadsworth Publishing Co. Inc. Belmont, California. https://search.worldcat.org/title/1345492694 .
12. Jeans, Sir James (1936) How the Moon will disintegrate. Nenones Practical Machines.
13. Moore, Patrick (1992) Fireside Astronmy: An Anecdotal tour through the history and lore of Astronomy. John Wiley & Sons. https://collection.sciencemuseumgroup.org.uk/documents/aa110073544/fireside-astronomy-an-anecdotal-tour-through-the-history-and-lore-of-astronomy.
14. Garlick Mark A (2002) The Fate of Earth. Sky & Telescope 30-35.
15. Sharma, Bijay Kumar (2023C) The Past, Present and Futuristic Earth Moon Orbital-Globe Dynamica and its habitability. Journal of Mathematical Techniques and Computational Methods 2: 48-66.
16. Zhang, Junjum, Dauphas, Nicolas, Davis, et al. (2012) The proto-Earth as a significant source of Lunar Material Nature GeoScience 5: 251-255.
17. Cuk, Malija, Stewart, Sarah T (2012) Making the Moon from a fast spinning Earth: A giant Impact followed by resonant despinning. Science 308: 1047-1052.
18. Kaula, William K (1969) The Gravitational Field of the Moon. Science 166: 1581-1588.
19. Cameron AGW (2002) Birth of a Solar System. Nature 418: 924-925.
20. Kerr R A (2002) The First Rocks Whisper of their Origins. Science 298: 350-351.
21. Toubol M, Kliene T, Bourdon B, Palme H, Wiele R (2007) Late formation and prolonged differentiation of the Moon inferred from W isotopes in Lunar Metals. Nature 450: 1206-1209.
22. Stevenson J, David (2008) A planetary perspective on the deep Earth. Nature 451: 261-265.
23. Maddox J (1994) Future History of our Solar System. Nature 372: 611.
24. Halliday A N, Wood B J (2007) Treatise on Geophysics. 9: 13-50.
25. Chambers, John E (2004) Planetary Accretion in the inner Solar System. Earth and Planetary Science Letters 223: 241-252.
26. Raymond S N, Mandell A M, Siggurdson S (2006) Exotic Earths forming habitable worlds with giant plant migration. Science 313: 1413-1416.
27. Ogihara M Ida S, Morbidelli A (2007) Accretion of terrestrial planets from oligarchs in a turbulent disk. ICARUS 188: 522-534.
28. Lissauer JJ, Stevenson D J (2007) Protostars and Planets V, (eds. Reipurth, B, Jewitt D. & Keil, K.) 591-606.
29. Gomes R, Levison H F, Tsiganis K, Morbidelli A (2005) Origin of the cataclysmic Late Heavy Bombardment period of the terrestrial planets. Nature 435: 466-469.
30. Canup R M, Esposito (1996) Accretion of the Moon from an impact generated disk. ICARUS 119: 427-446.
31. Sharma, Bijay Kumar (2023) High Obliquity, High Angular Momentum. Earth as Moon's Origin revisited by Advanced Kinematic Model of Earth-Moon System. Journal of Geography and Natural Disasters 13: 1-11.
32. Cameron AGW (2001) From interstellar gas to Earth-Moon System. Meteoritic Planetary Science 36: 9-22.
33. Canup RM (2004) Simulations of late lunar forming impact, Icarus 168: 433-456.
34. Reufer A, Meier MMM, Benz W, Wider R (2011) Obtaining higher target material proportion in giant impact by changes in impact parameter and impact composition. Lunar Planetary Science Conference 42: 1136
35. Genstenkorn H (1955) Uber Gezeitenreibung beim Zweikarpenproblem. Z Astrophysics 26: 245-274.
36. Macdonald GJF (1964) Tidal Friction. Review Geophysics 2: 467-541.
37. Kaula WM (1964) Tidal dissipation by Solid friction and the resulting orbital evolution. Review Geophysics 2: 661-684.
38. Rubicam DP (1975) Tidal Friction & the Early History of Moon's Orbit. Journal of Geophysical Research 80: 1537-1548.
39. Touma J, Wisdom J (1998) Resonances in the Early Evolution of Earth-Moon System. The Astronomical Journal 115: 1655-1663.
40. Williams DM, Kasting JF, Frukes LA (1998) Low-Latitude glaciation and rapid changes in the Earth's Obliquity explained by obliquity-oblateness feedback. Nature 396.
41. Ward WR, Canup RM (2000) Origin of the Moon's orbital inclination from resonant disk interactions. Nature 403: 741-743.
42. Touma J, Wisdom J (1994) The Astronomical Journal. https://adsabs.harvard.edu/full/1994AJ....108.1943T.
43. Goldreich P (1966) History of Lunar Orbit. Review of Geophysics 4: 411-439.
44. Cameron AGW (1997) The Origin of the Moon & the Single Impact Hypothesis. ICARUS 126: 126-137.
45. Benz W, Slattery WL, Cameron AGW (1986) The Origin of the Moon & the Single Impact Hypothesis. ICARUS 66: 515-535.
46. Benz W, Slatery WL, Cameron AGW (1987) The Origin of the Moon & the Single Impact Hypothesis. ICARUS 71: 30-45.
47. Melosh HJ, Kipp ME (1989) Lunar Planetary Science Conference XX 685-686.
48. Kipp ME, Melosh HJ (1986) Origin of the Moon, edited by Hartmann. Phillip and Taylor 643-647.
49. Canup RM, Asphaug Erik (2001) Origin of the Moon in a giant impact near the end of the Earth's formation. Nature. https://www.lpl.arizona.edu/~shane/PTYS_554_2017/reading/Canup_Nature_2001.pdf.
50. Williams, George E (2000) Geological Constraints on the Precambrian History of Earth's Rotation and the Moon's Orbit. Review of Geophysics 38: 37-59.
51. Leschiutta S, Tavella P (2001) Reckoning Time, Longitude and The History of the Earth's Rotation, Using the Moon Earth. Moon and Planets 85: 225-236.
52. Krasinsky GA (2002) Dynamical History of the Earth-Moon System. Celestial Mechanics and Dyanical Astronomy 84: 27-55.
53. Cook CL, Dukla JJ, Cacioppo R, Gangopadhyaya A (2005) Comment on Gravitational Slingshot by American. Journal of Physics 72: 619-621.
54. Dukla JJ, Cacioppo R, Gangopadhyaya A (2004) Gravitational slingshot. American Journal of Physics 72: 619-621.

55. Epstein KJ (2005) Shortcut to the Slingshot Effect. American Journal of Physics 73: 362.
56. Jones JB (2005) How does the slingshot effect work to change the orbit of spacecraft? Scientific American 116.
57. Sharma BK (1995) Theoretical Formulation of Earth-Moon System revisited. Proceedings of Indian Science Congress 82nd Session Jadavpur University. Calcutta 17.
58. Sharma BK, Ishwar B (2002) Lengthening of Day curve could be experiencing chaotic fluctuations with implications for Earth-Quake Prediction. World Space Congress-2002 Houston Texas USA 3.
59. Sharma BK, Ishwar B (2004) Planetary Satellite Dynamics: Earth-Moon, Mars-Phobos-Deimos and Pluto-Charon (Parth-I) 35th COSPAR Scientific Assembly, 18-25th July 2004A, Paris, France.
60. Sharma BK, Ishwar B (2004) Jupiter-like Exo-Solar Planets confirm the Migratory Theory of Planets Recent Trends in Celestial Mechanics 225-231.
61. Sharma BK (2011) The Architectural Design Rules of Solar Systems based on the New Pespective. Earth, Moon and Planets 1: 15-37.
62. Zahn (2012) Present State of Tidal Theory. Binaries as Tracers of Stellar Formation, Edited (1992) by A Duquennoy & M Mayor Cambridge: Cambridge University Press 401: 265-268.
63. Claret AL, Cunha NCS (1997) Circularization and Synchronization times in Main Sequence of detached eclipsing stars:II Using formalisms of Zahn. Astronomy & Astrophysics 318: 187-197.
64. Sharma, Bijay Kumar (2023) Iapetus hypothetical Sub-satellite revisited and it reveals celestial body formation in Primary centric Framework. Journal o Research and Development 11: 1-16.
65. Parsons SG, Marsh TR, Coperwheat CM, Dhillon VS, Littlefair SP, et al. (2009) Precise Mass and Radius values for the White Dwarf and Low Mass M Dwarf Star in the pre-cataclysmic binary NN Serpentis. Monthly Notices of Royal Astronomical Society 000: 1-20.
66. Lacy, Claud H (2025) Sandberg; Torres, Guillermo: Claret, Antonio; and Vaz, Luiz Paulo Ribeiro Absolute Properties of the Eclipsing Binary Star RW Lacertae. The Astronomical Journal 130: 2838-2846.
67. Sean O'Brian M, Howard E Bend (2001) Hubble Space Telescope Spectroscopy of V471: Oversized K Star, Paradoxical White Dwarf. Ap J 563: 971-986.
68. Denoghnue DO, Koen C, Kilkemy D, Stobie RS, Koester D, et al. (2003) The DA+dMe eclipsing binary EC 13471-1258: its cup runneth over…. kust. Monthly Notices of Royal Astronomical Society 345: 506-528.
69. Goldreich, Peter, Soter, Steven (1966) Q in Solar System. 5: 375-389.
70. Gladman, Brett QuinnD, Dane Nicholson, Phillip, Rand, et al. (1992) Synchronous Locking of tidally Evolving Satellites 122: 166-192.
71. Prodan, Snezana, Murray, Norman (2011) On the dynamics & tidal dissipation rate of the White Dwarf in 4: 1820-1830.
72. Bloom, Joshua S, Giannios, Dimitrios, Metzger, et al. (2011) A possible Relativistic Jetted Outburst from a Massive Black Hole fed by a tidally disrupted Star. Science 333: 203-206.
73. Oakes, Kelly (2011) We are cosmic dust but you are everything to me. Scientific American.
74. Damour, Thibault (1992) Binary Pulsars as Probes of Relativistic Gravity. Philosophical Transactions of Royal Society of London: Physical Science and Engineering 341: 135-149.
75. Tiec AL, Mroue AH, Barack L, Harald P Pfeiffer, Norichika Sago et.al. (2011) eriastron Advance in Black Hole Binaries. 107: 141101.
76. Stairs, Ingrid H (2003) Testing General Relativity with Pulsar Timing. Living Reviews in Relativity, Published by Max Planck Institute for Gravitational Physics.
77. Wolszcyan A (1997) Relativistic Binary Pulsars. Relativistic Gravitation and Gravitational Radiations: Proceedings of Contemporary Astrophysics, Edited by Marck, Jean-Alain; Laota, Jean Pieere, Cambridge University Press https://iopscience.iop.org/article/10.1088/0264-9381/11/6A/017/pdf .
78. Backer DC, Kulkarni SR, Heiles C, Davis M.M, Goss WM, et.al. (1982) A Milli Second Pulsar. Nature 300: 615-618.
79. Rawley LA, Taylor JH, Davisc MM, Allan DW (1987) Millisecond pulsar PSR 1937+21: a highly stable clock. Science Wah 238: 761-765.
80. Goldreich P, Julian WH (1969) Pulsar Electrodynamics 157: 869-880.
81. Sturroc PA (1971) A model of Pulsars. Ap J 164: 529-556.
82. Taylor JH (1992) Pulsar Timing and Relativistic Gravity. Philosophical Transactions of Royal Society of London:Physical Sciences and Engineering 341: 117-134.
83. Barker BM, RF O Connell (1975) Astrophys J 199: 25.
84. Damour T, Ruffini R (1974) C.r.hebd.Seanc.Acad.Sci. Paris A 279: 971.
85. Taylor JH, Weisberg JM (1989) Further Experimntal Tests of Reltivistic Gravity using binary pulsars 345: 434.
86. Taylor JH, Wolszczan A, Damour T, Weisberg JM (1992) Experimental constraints on strong-field relativistic Gravity. Nature Lond 355: 132-136.
87. Lattimer, JM, Praksh M (2004) The Physics of Neutron Stars. Science 304: 542-546.
88. Manchester RN (2004) Observational Properties of Pulsars. Science 304: 542-546.
89. Bhattacharya D, Van Den Heuvel EPJ (1991) Phys Rep 203: 1-2.
90. Bisnovatyi-Kogan GS, Komberg BV (1074) Sov. Astron 18: 217.
91. Shibazaki N, Murakami T, Shaham J, Nomoto K (1989) Does mass accretion lead to field decay? Nature 342: 656.
92. Arzoumanian Z, Cordes JM, Wasserman I (1982) Pulsar Spin Evolution, Kinematics and Birth Rate of Neutron Star Binaries. Ap J 520; 696-705.
93. Verbunt F (1993) Origin and Evolution of X-Ray Binaries and Binary Radio Pulsars. ARA&A 31: 93-127.
94. Van Den Heuval EPJ, Kaper L, Ruymaekers E (1994) Cygnus X-3, PSR 2303+46 and the Origins of Double Neutron Stars. New Horizons of X-Ray Astronomy, First Results from ASCA. Proceedings of the International Conference on X-ray Astronomy held March 8-11.
95. Weisberg Joel M, Taylor JH (2002) The Relativistic Binary Pulsars B1913+16. Radio Pulsars. https://arxiv.org/abs/astro-ph/0211217.
http://www.johnstonarchive.net/relativity/binpulsar.html.
96. Bildstem Lars, Curt Cutlar (1992) Tidal Interactions of in-spiraling compact binaries. Ap J 470:175-180.
97. Lyne AG, Burgey M, Kramer M, Possenti A, Manchester RN, et al. (2004) A Rare Laboratory for Relativistic Gravity and Plasma Physics. Science 303: 1153-1157.
98. Burgay M, Amico ND, Possenti A, Manchester RN, Lyne AG, et al. (2003) An increased estimate of the merger rate of double neutron stars from observations of a highly relativistic

system. Nature 426: 531-533.

99. Deich WTS, Kulkarni SR, Van Paradijs J, Van Del Heuvel EPJ, et al. (1996) The Masses of the Neutron Stars in M15C. in eds Proceedings of the 165th Symposium of the International Astronomical Union: Compact Stars in Binaries 279-285.
100. Vollmann, Wolfgang (1993) Measurements of 61 Cygni (STF 2758AB, WDS 21069+3845). Journal of Double Star Observation 4.
101. Pourbaix D, Nidever D, McCarthy C, Butler RP, Tinney CG, et al (2002) Constraining the difference in convective blueshift between the components of alpha centauri ewith precise radial velocities. A & A 386: 208-285.
102. Boss Alan P (1998) Astrometric Signatures of giant planet formation, Nature 393: 141-143.
103. Sharma BK, Ishwar B, Rangesh N (2009) Simulation Software for the spiral trajectory of our Moon. Advances in Space Research 43: 460-466.
104. Alley CO, Bendu PL, Dicke RH, Faller JE, Franken PA, et al. (1965) Optical Radar Using a Corner Reflector on the Moon. Journal of Geophysical Research (all sections) 70: 2269.
105. Cox A (1999) Allen's Astrophysical Quantities. 4th Edition Springer-Verlag New York.
106. Damour T, Deruelle N (1986) General relativistic celestial mechanics of binary systems. II The post-Newtonian timing formula. Ann Inst H Poincar´e (Phisique Th´eorique) 44: 263-292.
107. Deakin RE, Hunter MN (2010) Geometric Geodesy Part A. https://www.mygeodesy.id.au/documents/Geometric%20Geodesy%20A(2013).pdf.
108. Dickey JO, Bender PL, Faller JE, Newhall XX, Ricklefs RL, et al. (1994) Lunar Laser Ranging: A Continuing Legacy of the Apollo Program. Science 265: 482-490.
109. Faller JE, Winer I, Carrion W, Johnson TS, Spadin P, et al. (1969) Laser Beam Directed at the Lunar Retro-Reflector Array: Observation of the First Returns. Science 166: 99.
110. Lyne AG, Camilo F, Manchaster RN, Bell JF, Kaspi VM, et al, (2000) The Parkes Mutibeam Pulsar Survey:PSR J1811-1736 a pulsar in a highly eccentric system. Monthly Notices of Royal Astronomical Society 312: 698-702.
111. Nice DJ, Sayer RW, Taylor JH (1996) PSR J1518+4904: A Mildly Relativistic Binary Pulsar System. Ap J 466: 87-90.
112. Peters PC, Mathews J (1963) Gravitational Radiation from point masses in Keplerian Orbit. Physical Review 131: 435-440.
113. Stairs IH, Thorsett SE, Taylor JH, Wolszczan A (2002) Studies of the Relativistic Binary Pulsar PSR B1534+12: I. Timing Analysis. Astrophys J 581: 501-508.
114. Wolszczan A (1991) A nearby 37.9 ms radio pulsar in a relativistic binary system. Nature 350: 688-690.
115. Zharkov VN (2000) On the history of the lunar orbit. Astronomichesky Vestnik 34: 3-14.